

University of Louisville

ThinkIR: The University of Louisville's Institutional Repository

Electronic Theses and Dissertations

5-2017

Development of a directional bone reaming system.

Richard J Ackermann
University of Louisville

Follow this and additional works at: <https://ir.library.louisville.edu/etd>



Part of the [Biomedical Devices and Instrumentation Commons](#)

Recommended Citation

Ackermann, Richard J, "Development of a directional bone reaming system." (2017). *Electronic Theses and Dissertations*. Paper 2819.
<https://doi.org/10.18297/etd/2819>

This Master's Thesis is brought to you for free and open access by ThinkIR: The University of Louisville's Institutional Repository. It has been accepted for inclusion in Electronic Theses and Dissertations by an authorized administrator of ThinkIR: The University of Louisville's Institutional Repository. This title appears here courtesy of the author, who has retained all other copyrights. For more information, please contact thinkir@louisville.edu.

**DEVELOPMENT OF A DIRECTIONAL BONE REAMING SYSTEM:
AN INNOVATION IN INTRAMEDULLARY REAMING**

By

Richard Joseph Ackermann III

B.S., University of Louisville, 2015

A Thesis

Submitted to the Faculty of the

University of Louisville

J.B. Speed School of Engineering

as Partial Fulfillment of the Requirements

for the Professional Degree

MASTER OF ENGINEERING

New Product Development

Department of Bioengineering

May 2017

Directional Reaming of the Intramedullary Canal:
An Innovation in Intramedullary Shaping

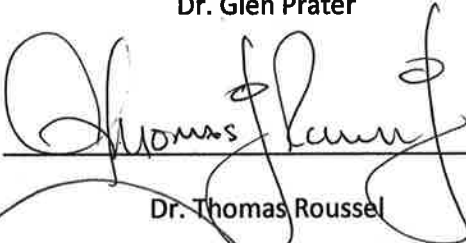
Submitted by: 
Richard Joseph Ackermann III

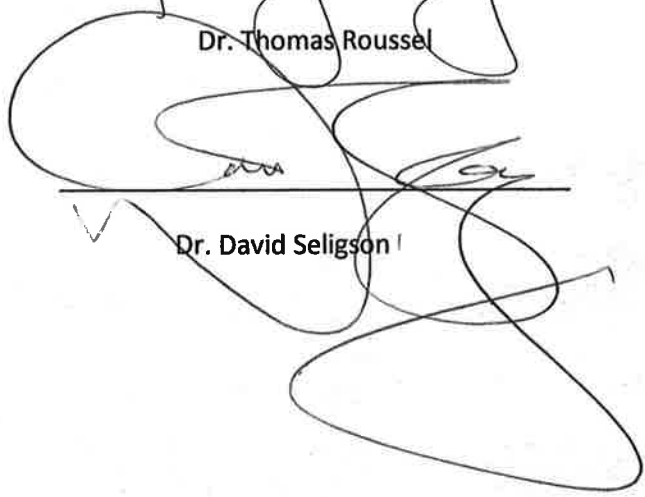
A Thesis Approved on
28 APRIL 2017

By the Following Reading and Examination Committee:


Dr. Michael Voor: Thesis Advisor


Dr. Glen Prater


Dr. Thomas Roussel


Dr. David Seligson

Acknowledgements

A sincere appreciation is extended to all who assisted the candidate in the completion of the project. These individuals were vital in providing funding, facilities, and support for the candidate's success through the duration of the project.

The author would like to acknowledge the following groups and individuals:

- University of Louisville Fresh Tissue Laboratory
- University of Louisville Health Science Campus Machine Shop
- The University of Louisville's Biomedical Engineering Department
- The Coulter Foundation
- East End Import Services, LLC
- First Build
- Devicix LLC
- Dr. David Seligson M.D.
- Dr. Michael Voor

Abstract

Preparation of long bones such as the femur or tibia for placement of intramedullary devices for the treatment of fractures usually involves reaming with a series of central cutters driven by a drill-like device with a flexible shaft over a guide wire. The reamers sequentially enlarge the intramedullary canal into a tunnel of circular cross-section and a diameter appropriate for the procedure. The current technology is concentric, meaning that the system is self-centering within the original intramedullary canal and the expansion is symmetric with respect to the original centerline. A novel system for laterally deflecting the head of a 12mm Stryker Bixcut reaming system has been designed in order to test the proof of concept for eccentrically reaming the intramedullary canal of a long bone. Reaming often precedes intramedullary nail placement following a long bone fracture or to induce ankle arthrodesis. Long bones do not always contain a regularly shaped intramedullary canal, thus creating a risk in navigating a reamer through the bone. Pockets of infected tissue and malformed fractures may also create obstacles for advancing a reamer through the canal. The newly developed reaming system is intended to allow the surgeon to be more selective in where the reamer head cuts while shaping the inner wall of the intramedullary canal to avoid or target certain areas of the canal. Development of the directional reaming system included two prototypes with three sets of experiments to quantify the success of the designs. The first experiment resulted in a prototype unable to achieve the specified 3mm of lateral cutting depth. The second experiment also failed to achieve the 3mm of lateral cutting depth, but did yield a proof of concept driving the design of the third iteration. Creation of the third prototype concludes the project with experimentation that was completed in early May of 2017.

Contents

Acknowledgements	5
Abstract	6
I. Introduction	9
A. Potential Clinical Applications	10
a. Unusual or Irregular Anatomy.....	10
b. Use of Directional Bone Reamer in Nonunions and Malunions.....	13
c. Ankle Immobilization/Fusion (Arthrodesis) Using IM Nails.....	15
d. Nail Impingement of the Anterior Cortical Wall.....	17
e. Osteomyelitis in Directional Reaming	18
f. Reaming to Improve Vasculature after Surgery	20
B. Objectives	21
II. Directional Reaming System Prototype Development	23
A. Conical Bearing	23
B. Conical Insert	24
C. Follower Sleeve Development	27
D. Translating Reamer Prototype	30
a. Plunger design	31
b. Follower sleeve (Tube) and Plug Design.....	32
c. Body Design	32
III. Materials and Methods	34
A. First Prototype (12mm Conical Insert)	35
a. Devicix Experiment 1	35
B. Second Prototype (14mm Conical Bearing)	37
a. Devicix Experiment 2	37
b. Cadaver Experiment	42
C. Third Prototype (Translating System)	50
Sawbone Experiment.....	50
IV. Results	54
A. First Prototype (12mm Conical Insert)	54
B. Second Prototype (14mm Conical Bearing)	55
Third Prototype (Translating System)	61

V. Discussion	64
VI. Conclusion	66
Appendix A: Prototype Prints and CAD Drawings	68
Appendix B: Design Calculations	71
Appendix C: Prototype Development Procedures	75
Appendix D: Follower Sleeve Finite Element Analysis Report	83
Appendix E: Cadaver Trial 1 Fluoroscopic X-rays	95
Appendix F: Miscellaneous Information	98
List of Figures	0
References	4

I. Introduction

Reaming is generally used to expand an intramedullary (IM) canal for implantation of a stabilizing nail for the fixation of fractures of long bones such as the tibia or femur. While the benefits and drawbacks of reaming before nail insertion are still contested, it is known that stability increases with nail size[1]. Therefore, reamers are commonly employed to optimally increase the diameter of the IM canal for the appropriate nail. In addition to increasing stability of fracture treatment, reaming has been shown to allow for the release of certain osteogenic elements such as transforming growth factor-beta and pluripotent stem cells. Healthy bone grafting material can also be salvaged with the incorporation of a reamer irrigator-aspirator system. [2]

A typical reaming system is composed of a cannulated driving apparatus, either pneumatic or electric, a guidewire, and a flexible reaming shaft and attached reamer head permanently fixed to the shaft or with a modular head attachment for interchangeable sizes. Reaming and nail insertion can be done antegrade (proximal to distal) or retrograde (distal to proximal) depending on the fracture type, the bone involved, and the nail to be used. In a standard reaming procedure, the guidewire is first inserted into the intramedullary canal through an opening created in one end of the bone and embedded into the opposite end of the bone. Next, the reaming assembly is placed over the guidewire and inserted into the canal. Reamer head sizes are chosen depending on the size of the bone and the diameter of the nail being inserted and often are used to expand the intramedullary canal in .5mm increments to 1-1.5mm larger than the nail diameter.

The objective of this project was to develop and test a prototype reamer that has the unique ability to ream laterally at specified positions along the length of the long bone. This technique should be as similar as possible to the standard reaming process, but allow for targeted widening of the intramedullary canal for a variety of clinical purposes.

A. Potential Clinical Applications

Reaming of long bones has become a well-established practice in the reduction of long bone fractures, treating malalignments, and pseudarthroses [1, 3]. Reaming may also be used to remove necrotic or infected tissue within the intramedullary canal as well as create bone grafting chips for packing into fractured sites with the use of the reaming irrigator/aspirator systems now commonly employed in the reaming process[4]. In each of these circumstances, the ability to guide the reamer without being forced to follow the native intramedullary geometry would be advantageous for several reasons.

a. Unusual or Irregular Anatomy

The medullary cavity is not always regularly shaped or centrally located within the long bone. After a fracture, bone fragments may not always heal in the correct orientation causing irregular geometries, or they may heal only partially or not at all. With the proposed directional reamer system, one would be able to more accurately remove targeted bone within the canal instead of simply following the original curved pathway within the bone and risking the bones' structural integrity during the healing process.



Figure 1[5]: A healed tibia two years after fracture operation is shown on the left with a prospective need for directional reaming system to more accurately follow the intramedullary canal in comparison to a healthy tibia on the right.

Figure 1 shows a tibia that has healed to a stable weight-bearing (although irregular) structure after a closed fracture; however, due to a malunion as well as infection and osteonecrosis, a second operation involving an Ilizarov/Taylor Spatial Frame was necessary. While the case from which the X-ray in **Figure 1** was taken healed to a weight bearing structure, it offers a perfect example of why a directional reaming system could be advantageous in following an irregularly shaped IM canal. Cases associated with open fractures treated with intramedullary nails are prone to develop infection [6, 7] giving rise to a need for improvements within the reaming process for nail insertion. A system allowing the surgeon to direct of the position of the reamer head while inside the intramedullary canal would allow for a more controlled region of the bone to be reamed. This in turn could create a closer fit between the intramedullary nail and the native curvature of the bone, reducing the chances of non-

union, malunion, and possibly deep tissue infections. It could also introduce innovation in the field of optimizing nail shape for providing support in fracture cases. The adult femur is curved with an anterior bow with an average radius of curvature of $1.17 \pm 0.3\text{m}$ to $1.21 \pm 0.27\text{m}$ [8, 9]. This curvature can sometimes introduce risk in the form of anterior encroachment of the femoral cortical wall when inserting an antegrade intramedullary nail most often during pertrochanteric or subtrochanteric fracture treatment. While this complication is not common, it does present a potential need for altering the curvature of the intramedullary canal to assist in choosing the appropriate nail. The new system must also have the ability to flex and follow the native curvature of the bone while maintaining the ability to transfer the appropriate amount of torque from the rotational driver to the reamer head.



Figure 2: An anterior view of a tibial fracture is shown with an associated fibula fracture. A reamer system and guidewire across the fracture site enable reduction of the tibia fracture. Use of a directional system in this case would allow for a more accurate navigation of the fracture site increasing the success rate of the operation.

Notice in **Figure 2** that though the tibial fracture has been reduced using external pressure and the guidewire, the reamer is still at risk for being off of the central axis of the IM canal in the distal

fragment. Correct alignment of the guidewire and reamer is critical since it determines the nail placement and subsequent success of the operation. As the reamer approaches the fracture site, greater control of the cutting head would give the surgeon the ability to more easily align the proximal and distal sections of bone. In the event of a diaphyseal nonunion or malunion, it may be necessary to reshape the intramedullary pathway particularly if an operation such as a clamshell osteotomy will be performed to maintain the natural curvature of the bone. This type of osteotomy involves removing a grossly deformed section of the diaphysis, cutting the affected location usually axially, and then replacing it in an orientation that maintains a more normal anatomical position and physiology. A malformed tibia that has undergone an ideal clamshell osteotomy is illustrated in **Figure 3**. A laterally deflecting reamer system may aid in conducting such a procedure by allowing the surgeon to be more selective in areas of the malformed canal that require substantial cortical support.

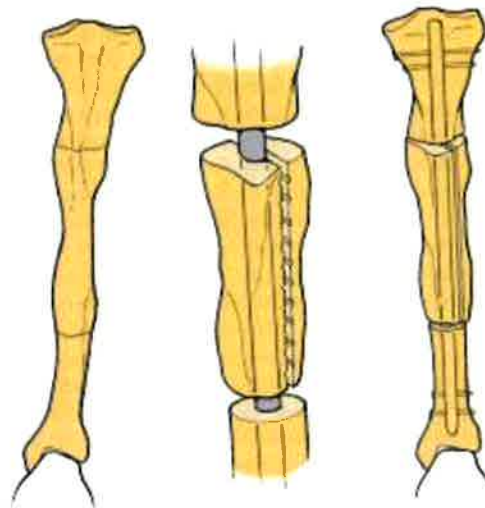


Figure 3: A clamshell osteotomy is illustrated above. A segment of the shaft is extracted, cut, and replaced to form a more normal anatomical position.

b. Use of Directional Bone Reamer in Nonunions and Malunions

A nonunion is defined as a fracture that has failed to heal after one year from the initial surgery or has needed repeated surgeries to treat the fracture. If allowed to progress without treatment, a nonunion with no chance of fusing may be perceived by the body as a false joint, and even develop

rounded edges along the bony interface imitating an articular surface commonly referred to as pseudarthrosis. A malunion occurs in areas of malalignment between healed surfaces of bone and requires readjustment of the bone segments to correct alignment during the healing process. While the exact mechanism of nonunion and malunion development is still debated, it is known that they are generally preventable by following three principles when setting a long bone fracture. They are as follows: minimize gap between fractured faces, provide adequate blood flow and nutritional supply to fracture site, and stabilize the fracture site to prevent inadvertent movement of the fractured bones [10]. Nonunions and malunions are also more commonly associated with open fractures than closed fractures. Treatment of open fractures is also associated with higher chances for deep infection than closed treatment due to increased exposure to the compromised environment. Nonunions and malunions are divided into two categories: hypertrophic and atrophic. Hypertrophic nonunions and malunions develop due to insufficient reduction or stability of the fractured area and may cause irregular bone reconnection and osteophyte formation [6]. Atrophic nonunions are generally caused by severe loss of osteogenic activity. It may also be induced as a result of extreme vascular destruction around the fracture site, fracture defects, or infection.

Both atrophic and hypertrophic nonunions are breeding grounds for bacteria and common sites for necrosis (tissue death). Treatment involves the removal of the infection and necrotic tissue primarily using antibiotic treatment and complementary debridement in more extreme cases[6]. Due to the irregular geometry of the intramedullary canal resulting from the diseased conditions, it may not always be practical or safe to use a conventional reaming treatment to remove the infected or necrotic bone. Thus, use of the new_directional system would offer a more controlled method of preserving healthy osseous tissue while removing infected areas without invasively excising sections of the bone.

c. Ankle Immobilization/Fusion (Arthrodesis) Using IM Nails

Ankle arthrodesis may be employed for a variety of reasons; some of which include severe arthritis, Charcot neuropathy, avascular necrosis, failed arthroplasty, and pseudarthrosis. Depending on the condition, several methods of joint immobilization as treatment options[11] exist; however, most methods include the use of either retrograde or antegrade intramedullary nail. Two key steps in achieving a successful ankle fusion using an IM nail are tibiotalar articular debridement and correct alignment of the tibial IM canal and the central axis of the talocalcaneal joint. Formal subtalar and tibiotalar articular debridement are recommended to promote successful union, but it adds a significant amount of time to the surgery and increases the damage done to the surrounding soft tissue[12]. Implementation of an innovative directional system for intramedullary reaming may reduce the need for such extensive debridement by more directly locating the medial regions of the calcaneus and talus without compromising the soft tissue capsule.

Complications of ankle arthrodesis using IM nails can result if proper anatomical alignment is not achieved or if joint stability is insufficient. Much of the risk of malalignment can be avoided with correct placement of the guidewire, but it is still possible that the nail inserted over the guidewire may be slightly off center. Hyer et al. [13] demonstrated the importance of guidewire placement for use in a retrograde nailing procedure in the hindfoot. Ten cadavers were used to observe placement of guidewires in an antegrade fashion into the tibial canal and measure their location relative to the central axis of the talus and calcaneus. From the study, it was found that even when the guidewire was placed successfully along the central axis of the tibial IM canal, seven of the ten guidewires moved lateral to the central axis as shown in **Figure 4** below, and missed the medial regions of the talus and calcaneus which are necessary for a stable anchoring of an IM nail. Damage to the talocalcaneal joint may occur leading to insufficient nail stability which, in turn, may lead to a nonunion. In addition to joint damage, the nail may be inserted into the tibia off-center. This may result in a nail that does not span completely into the

isthmus, or put the patient at risk for tibial fracture from a nail that may be the appropriate length if otherwise inserted in a centralized manner.

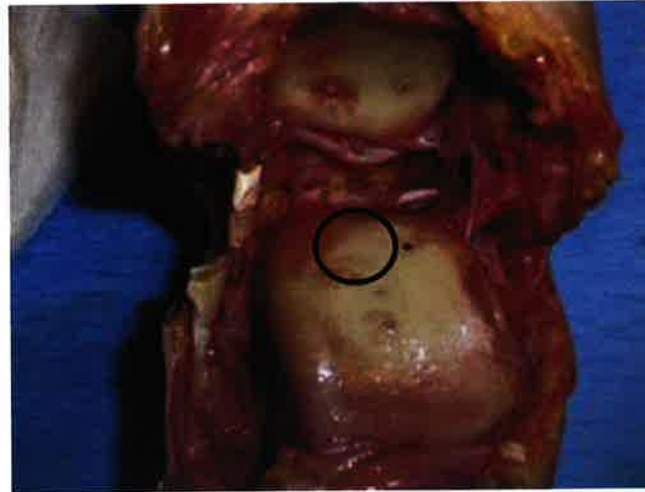


Figure 4 [13]: The dissected tibiotalar joint is shown above with the guidewire hole circled in black. Notice the location of the hole relative to the center of the talus. This image indicates the impending structural damage that may be caused to the talus and subsequently calcaneus once the reaming procedure for nail insertion begins.

Upon reviewing the effects of retrograde reaming on the subtalar and tibiotalar joints in cadavers, it has been observed that 5.89% of the posterior facet of the talus and 4.01% of the calcaneal facet sustains damage. Both medial facets suffered no damage though the guidewire placement was observed anteroposterior, laterally, and axially. For this reason, greater directional control of the reamer head would allow a more centralized cut through the medial region of the tibiotalocalcaneal joint for a more favorable nail placement as well as centralized placement within the tibial IM canal. It is proposed that the reaming system be inserted into the medial region of the joint then begin the directional reaming process to induce a valgus curved cut more closely matching the alignment of the calcaneus.



Figure 5: A lateral fluoroscopic radiograph from the study by Lowe et al. is shown depicting the location of a 12mm reamer at the tibiotalocalcaneal joint. By deflecting the reamer head posteriorly in this circumstance, less bending stress may be placed on the components of the talocalcaneal region as well as a better alignment may be achieved in order to more accurately enter the tibial IM canal ensuring optimal nail placement.

More recently developed ankle arthrodesis nails contain a valgus bending at the distal end for better alignment to calcaneal bone. This geometry is meant to reduce the neurovascular damage done to the plantar region of the foot and reduce the stress generated across the isthmus[14]. Matching the curvature of the nails when reaming would offer a significant advantage when inserting the nails and avoiding the plantar neurovascular bundle normally at risk when such an operation is conducted. The directional reamer system provides an ideal means to adjust the cutting angle once the reamer head has passed the talocalcaneal joint and enters the distal tibia to access the IM canal.

d. Nail Impingement of the Anterior Cortical Wall

While it is not an altogether common complication, cases also exist in which intramedullary nails have penetrated the anterior wall of the canal usually during antegrade placement. In cases such as cephalomedullary fixation, it is possible that the distal region of the nail may be placed either too close to the anterior cortical wall of the canal or puncture it leading to further complications such as pain or fracture. This intraoperative complication most often results from femoral curvature mismatch with the shape of the nail. However, certain anatomical factors may also contribute. In the average femur, the

intramedullary canal often approaches the anterior region of the distal femur[15]. Canal expansion also occurs with age due to decreasing bone density subsequently weakening the cortical wall's support for an intramedullary nail. Intraoperative factors may also contribute to anterior impingement such as erroneous nail entry, inadequate visibility during nail placement, and improper nail curvature.

One possible application of such a directional reaming device would be to mitigate the risk of femoral curvature/nail mismatch as described above. It could give the surgeon an advantage during preoperative planning in nail selection and assist in placement of nails within femurs containing irregular curvature. For example, using the directional reaming system to appropriately shape the canal would allow a nail with a smaller radius to be employed to avoid detrimental contact or perforation of the anterior wall of the intramedullary canal.

e. Osteomyelitis in Directional Reaming

Osteomyelitis is an inflammation of bone tissue caused by bacterial infections such as staphylococcus aureus, Escherichia coli, and Streptococcus pyogenes among others[16]. It most often develops from contaminated contact during surgical intervention, piercing injury, hematogenous contact, or a contiguous source of infection proximal to the bony tissue[17]. Osteomyelitis is often difficult to diagnose because of the vague symptoms associated with its onset such as chronic pain, benign and malignant tumors, and swelling. Symptoms may also arise as a result of the type of infection causing the osteomyelitis in addition to the general symptoms commonly associated. These symptoms include secondary suppurated infection, vascular congestion, cyst formation, bone pseudo-arthritis, bone trauma, and thrombosis. Unchecked vascular congestion and thrombosis in particular play a prominent role in advancing sequestration of the infected area.

Though necrosis is a common factor in both acute and chronic osteomyelitis, new bone deposition also occurs from surviving bone tissue within the infected area. This regrowth can surround the infected site enclosing the necrotic bone within the periosteum. This enclosure or involucrum may

increase in density and could restructure the surface of the bone as well as obstruct the intramedullary canal. Rather than excising the infected portion of the bone from the exterior of the cortical layer, removal of the infected or necrotic bone may be achieved by directing a reamer towards that location from the interior.

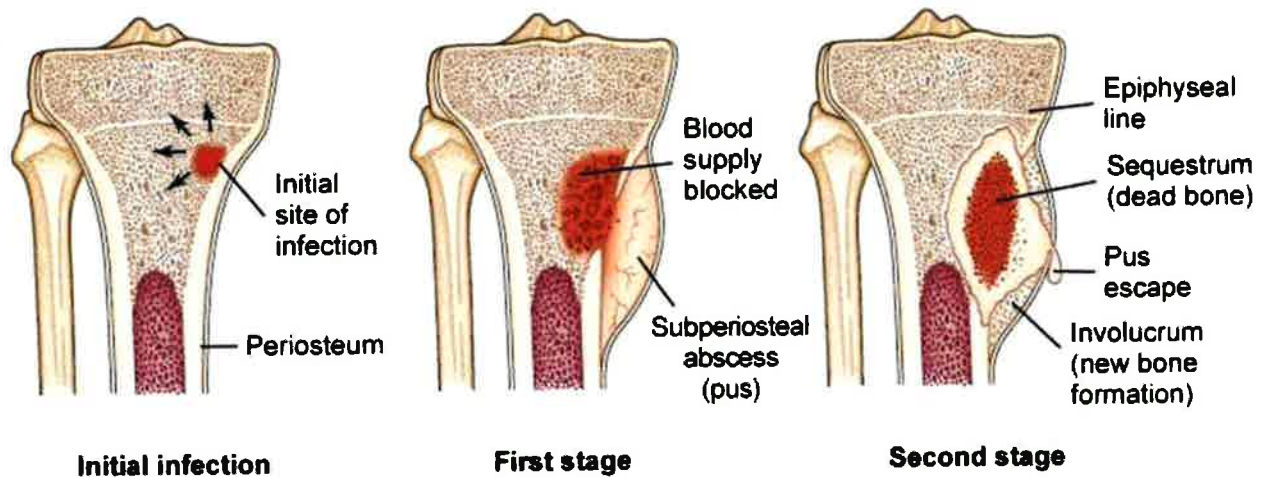


Figure 6[23]: Progression of osteomyelitis is illustrated in the figure above. Note the devascularization shown in the first stage which along with a biofilm formation greatly reduces effectiveness of antibiotic treatment. For this reason, surgical debridement is often necessary.

It is necessary to completely remove the infected tissue to effectively treat osteomyelitis.

Additionally, the intramedullary canal must be cleared if an implant (such as an IM nail) is to be inserted for long bone stabilization. While standard reaming may accomplish both tasks to a point, the irregularity of force loading and location of bone regrowth may require a more sculpted approach as can be inferred from **Figures 1 and 7**. The area called out by the black arrow in **Figure 7** is a necrotic pocket characteristic of advanced stages of repeated infection. Reaming laterally to concentrate on the affected area would give the surgeon the ability to more easily clear the infected site without compromising surrounding healthy bone in stages 2 and 3 of osteomyelitis development and possibly reducing the need to form an open excision of the infected tissue. Note the lesion depicted in **Figure 7** is shown to occur on the lateral side of the tibia and spans from the periosteum to the intramedullary canal. Though the occurrence of osteomyelitis in adults is decreasing, it still maintains a prominent existence in older

patients or patients with a chronically compromised immune system. It should also be noted that in addition to being difficult to diagnose early, 50% to 75% of the affected bony tissue will be compromised beyond repair before the lesion will be clearly visible to fluoroscopic imaging[18]. In these circumstances, it is imperative to remove the affected tissue with the most minimally invasive means possible.



Figure 7: Lateral Tibia of a 46-year old female showing a pocket of sequestrum as a result of repeated infection highlighted by the black arrow. Pockets such as the one shown pose a problem for standard reaming operations concerning the structural integrity of the cortical wall as the reamer head passes the infected site.[3]

f. Reaming to Improve Vasculature after Surgery

Reaming has been found to positively affect the healing process of bony tissue after a surgery as well as reduce the time to induce bone union [19, 20]. Specifically, reaming causes the release of certain osteogenic and angiogenic growth factors such as Transforming growth factor-beta ($TGF-\beta$) including the bone morphogenetic protein family, vascular endothelial growth factor (VEGF), and insulin like growth factor-1 (IGF-1) [1, 21-23]. Additionally, $TGF-\beta$ recruits mesenchymal stem cells to assemble at bone resorption sites where they differentiate into osteogenic elements [24]. Certain cells may also survive the reaming process and aid in increasing healing rate as well as bone formation[25, 26]. Multipotent stem cells including mesenchymal stem cells with the potential to differentiate into osteogenic or neuronal elements have been found to play a role in the healing process after reaming. It has also been

found that collagenase treated bone fragments (reamed debris) have the ability to create stem cells and maintain a capacity for differentiation [26]. The stem cells are hypothesized to originate in the cortical bone that has been cut away during reaming to provide a growing scaffold and source of future osteogenic cells. An irrigator/aspirator assembly mounted to the reamer driver is often used to collect the reamed tissue from which the osteogenic material may be isolated. Future modifications to the developed directional reaming assembly could complement the Reamer Irrigator/Aspirator (RIA) system and give the surgeon a more selective means of acquiring grafting material from the medullary as well as metaphysis and epiphysis of long bones. As a result, conventional grafting locations such as the iliac crests (posterior and anterior) may be spared without compromising bone density in those locations.

B. Objectives

A system to laterally cut a minimum of 3mm into the intramedullary canal was proposed by the University of Louisville's Chief of the Fracture Service, Dr. David Seligson. Two designs were considered initially with a third following several months into the project. The first design considered was an eccentrically centered reamer head mounted to a cam at the distal end of the flexible reaming shaft. The second design included a conical bearing added to the distal shaft of an existing Stryker Bixcut reamer system. The third and final design used an inclined plunger to cause lateral reamer shaft translation. In order to fund the project, the team acquired a grant from the Wallace H. Coulter Foundation for translational research. A third party manufacturing company, Devicix LLC, was recruited to generate or outsource prototype parts and preliminary test data as needed.

The project proceeded as follows: After funding was secured, the first design was abandoned in favor of the conical bearing design, because that design was compatible with existing Stryker technology and the overall goal of the project was to out-license the technology to an existing orthopaedic device company. By keeping the design as close as possible to and in coordination with the components of an

existing reamer system, it was believed that Stryker would be interested in reviewing the technology with an option to license it from the University.

After choosing to pursue the conical bearing and flexible follower sleeve design, the goals and timeline for the project were established. The final product resulting from the development of the directional reaming device contains the following objectives:

- Develop a system to ream/cut laterally into the wall of a 12mm diameter intramedullary canal (IM) of a long bone [femur] a minimum distance of 3mm from the long axis of the canal
- Induce a controlled amount of deflection at the reamer cutting surface using an external control mechanism
- Propose a user interface familiar to the orthopaedic surgeon minimizing the learning curve associated with incorporating the proposed device into their arsenal
- Create initial concept drawings for 12mm directional reaming system
- Construct working prototypes
- Complete dry and cadaver tests to qualify prototype success
- Proceed to steps for qualifying clinical use of the proposed directional reaming device

From the objectives listed above, the following set of design criteria was established:

- The system must achieve a minimum of 3mm of lateral displacement allowing the cutting head to reach a maximum cutting distance of 9mm from the central axis of the IM canal at any length along the canal
- The follower sleeve must allow sufficient bending and lateral deflection of the flexible reamer shaft
- All components must not exceed a maximum outer diameter of 12mm
- System must be able to flex to follow the natural curvature of an adult femur
- System must be compatible with existing reamer driver technology
- System must maintain biocompatibility of existing reamer technology, including the modular dovetail connection between the flexible shaft and the 12 mm reamer head
- Displacement of the reamer head must be controlled externally
- Reamer walking and chatter must be minimized within the system to have negligible effects
- Reamer torque and temperature values as well as intramedullary pressure must not exceed levels found to cause irreversible damage to the medullary or fat extravasation and emboli[21, 22, 27]
- The system designed should allow sufficient clearance of reamed debris
- The 4mm reamer shaft must be able to transfer sufficient torque from the reamer driver to the reamer head without mechanical damage

- System must not cause a temperature increase within the IM canal to cause thermal necrosis

II. Directional Reaming System Prototype Development

A. Conical Bearing

The basic concept of the conical bearing or conical insert design is that a cone added to the reamer drive shaft in the vicinity of the reamer head could be deflected laterally by advancing a sleeve down the shaft with a rigid tongue facing forward to “ride up” the cone and thus deflect the shaft (**Figure 8**). The dimensions of the conical bearing and follower sleeve were derived from cantilever beam

bending formulae. From the calculations performed, it was concluded that only 2.44mm of lateral deflection could be achieved with an 11.5mm diameter conical bearing and 30mm follower sleeve tongue. When using a 60mm follower sleeve tongue, 3.01mm of lateral deflection was calculated, however, wall impingement of the conical bearing would prevent full deflection from occurring.

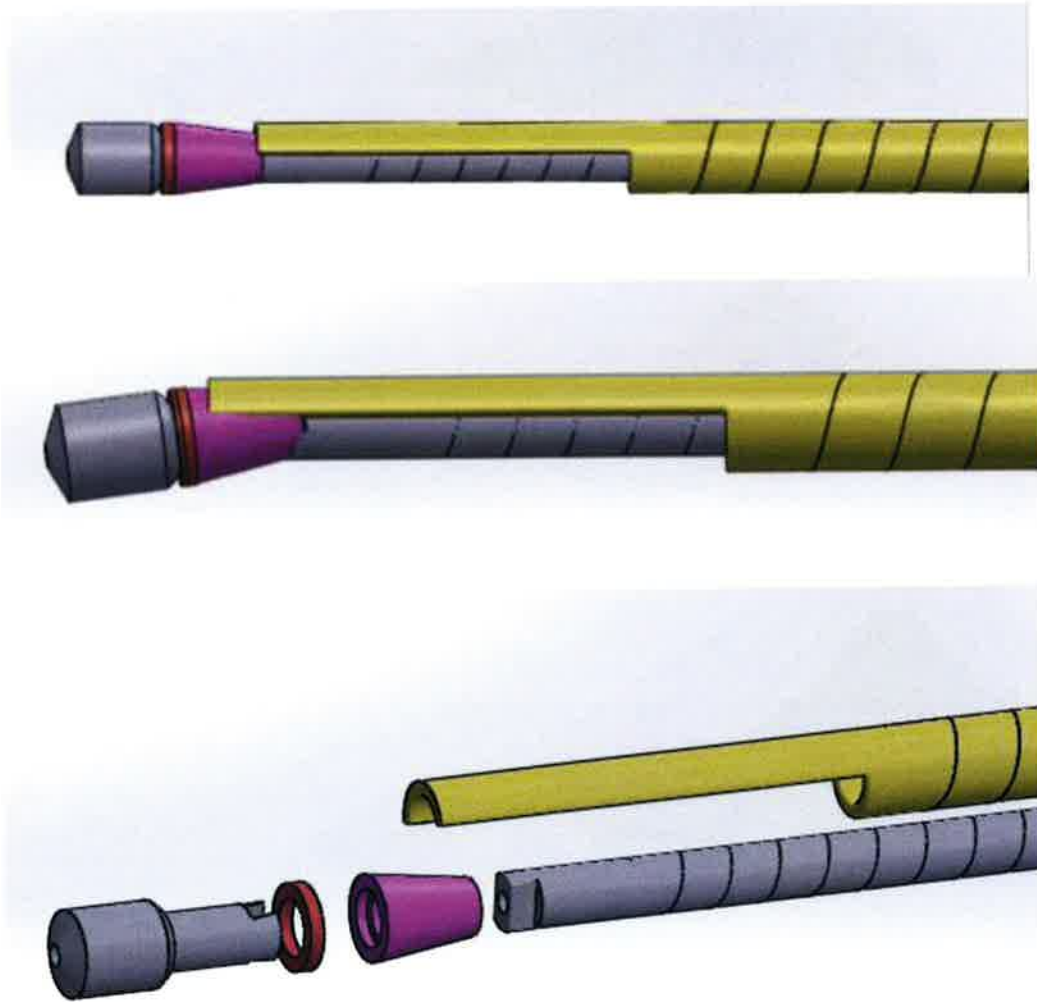


Figure 8: The 12mm conical bearing design is shown above. In this design, the follower sleeve (shown in yellow) is advanced over the conical bearing (purple) to force the flexible reamer shaft, illustrated as the gray spiral cylinder, to bend away from the follower sleeve's over hang thus deflecting the reamer head.

B. Conical Insert

Following the conical design, a conical dove-tailed insert to fit between a Stryker Bixcut flexible reamer shaft and 12mm reamer head was suggested by Devicix. This design, if it was proven to work, would be the best from a business development perspective because the additional part would fit directly with the existing Stryker reamer system simple by interposing the dove-tailed conical insert between the existing shaft and existing reamer head with requiring any modifications to those parts. The conical insert contained a shaft diameter of 8.0mm to match the flexible reamer shaft and a maximum conical diameter of 10.5mm. The added length of the insert was meant to provide a mechanical advantage in allowing a minimum of 3mm of lateral deflection while avoiding unwanted contact between the insert and inner diameter of the intramedullary canal. Conical inserts made of Polyether ether ketone (PEEK) and 316 stainless steel were manufactured for testing. Both materials were chosen for their use in surgical applications and biocompatibility. See **Figures 9 and 10** below:

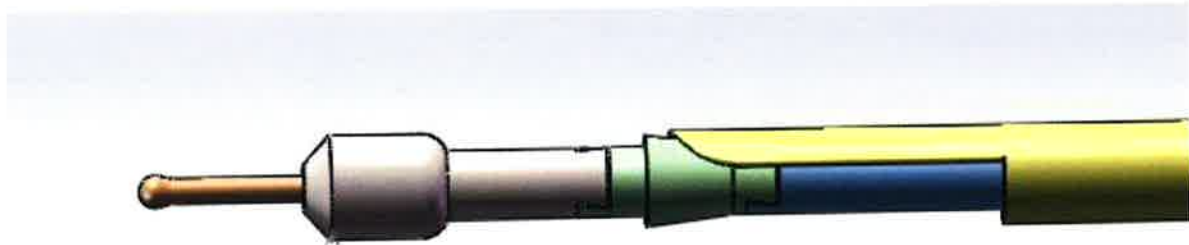


Figure 9: The conical insert design (green) is shown above. In this design, both peek and stainless steel inserts were manufactured as well as follower sleeves (yellow) in both materials.



Figure 10: the two follower sleeves and conical inserts are shown above. Experimentation has shown that deflected reaming has no damaging effects on either the peek or the stainless steel parts.

Conical Bearing (14mm)

A series of experiments completed at Devicix dictated the need for a design change away from the conical insert model resulting in the 14mm conical bearing assembly. The design change to a 14mm reamer head was deemed acceptable for prototyping purposes by the project’s resident orthopaedic surgeon for prototyping purposes. The mechanism for achieving reamer head deflection of the 14mm reamer head is similar to that of the conical insert design. However, instead of an insert, a conical bearing is secured axially by a press-fit connection onto the cylindrical section of the reamer head with an aluminum oxide blast to increase frictional resistance between the bearing and reamer head. The largest diameter of the conical bearing was calculated to be 13.25mm giving 2.625mm of deflection possible at the conical bearing (See **Appendix B**). This translates to 3.04mm of lateral deflection at the cutting head of the reamer. Unwanted contact between the IM canal wall and the flexible reamer shaft is still present if the reaming system is not advanced axially while the follower sleeve is being engaged

over the displacement bearing. This method of eccentric reaming will result in a wedge shaped trough in the inner wall of the intramedullary canal with a potential maximum cutting radius of 9.04mm.

C. Follower Sleeve Development

Development of the follower sleeve occurred in parallel to the deflecting conical bearing. The distal interface of the follower sleeve tongue has sustained two iterations that have been pursued to the level of manufactured prototypes. The first model of follower sleeve contained a 30mm tongue and was designed to accommodate the conical insert design described previously. A relief of 8.65mm was cut into the distal end of the sleeve to allow for a smooth engagement of the conical insert. A circumferential relief was created along the inner diameter of the tongue with a 10.6mm diameter as shown in the front view of the prints in **Appendix A**. The sleeve is 348mm in length which is suitable for a future external indexing attachment. Since this model of follower sleeve was meant only for preliminary testing, it was not designed to be flexible. Flexibility would be added to the follower sleeve after successful preliminary demonstrations. Peek and stainless steel were the materials chosen for the follower sleeve. There was initial concern that the peek components would sustain structural damage due to wear from the frictional force of the stainless steel – peek contact during rotation while the follower sleeve was advanced over the bearing. However, after the deflection experiment conducted at Devicix involving the conical insert segment, it was shown that the peek and stainless steel interface was sufficient and that there were negligible signs of wear on the peek follower sleeve when engaged over the stainless steel insert and the peek insert when deflected by the stainless steel follower sleeve.

The second sleeve prototype is designed to engage a conical bearing on the standard Stryker 8mm diameter flexible shaft in the same manner as the previous model; however the tongue is 30mm longer than the first prototype. This modification is meant to allow greater flexibility of the reamer shaft along the follower sleeve tongue. The tongue also only has the 10.6mm relief extending 20mm from the

distal edge. The remainder of the follower sleeve tongue contains an 8mm inner diameter to match the outer diameter of the reamer shaft. This aspect of the design is meant to limit reamer chatter and walking during deflected reaming as well as minimize machining cost. This prototype was also made flexible by means of quarterly slots cut perpendicularly to the axial length of the sleeve and alternating in the four quadrants (see **Figure 11**). The slots were cut using an electrical discharge machine (wire EDM). The number of slots was determined from an approximation of the bending stiffness of the Stryker Bixcut flexible reaming shaft and an FEA simulation in (see **Appendix B**). In order to isolate the bending stiffness (defined as EI , eqn. 8), the shaft was placed under four point bending using a Bionix 858 MTS machine. The amount of deflection (in millimeters) was used to track the amount of force placed on the shaft, and the moment created across the middle of the shaft was used to calculate the amount of deflection in a solid model of the flexible follower sleeve generated by finite element analysis using *SolidWorks 2015*. From this deflection, a bending stiffness was isolated and compared to that of the Stryker reamer shaft found from the MTS machine. The number of wire EDM cuts was then adjusted until the bending stiffness of the follower sleeve was 0.5010Nm which is sufficiently lower than the bending stiffness of the flexible shaft with a value of 0.6532Nm.



Figure 11: The distal end of the stainless steel follower sleeve with the slots cut for flexibility is shown above. It is important to note the relief cut into the distal portion of the tongue. This relief gives a smooth transition of the sleeve over the conical bearing when reaming laterally. The remainder of the tongue matches the outer diameter of the reamer shaft in order to add stability, provide a more economic manufacturing geometry, and minimize the chances of the reamer head walking or shaking during operation.

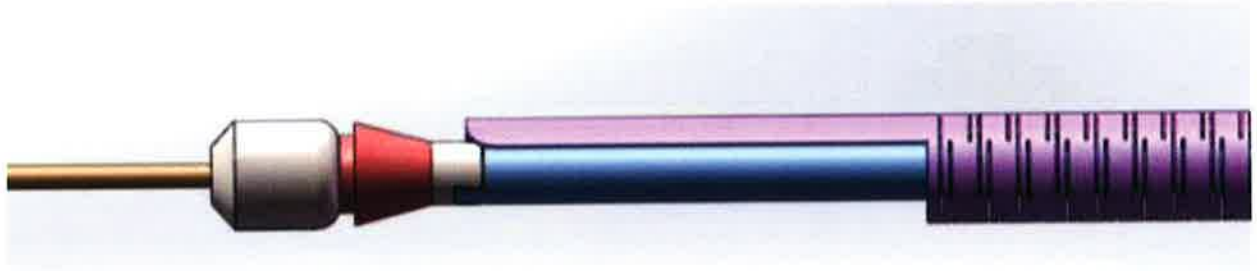


Figure 12: Shown above is the conical bearing and flexible follower sleeve design for the second round of testing. The flexibility slots can be seen in the right hand side of the assembly (shown in purple).

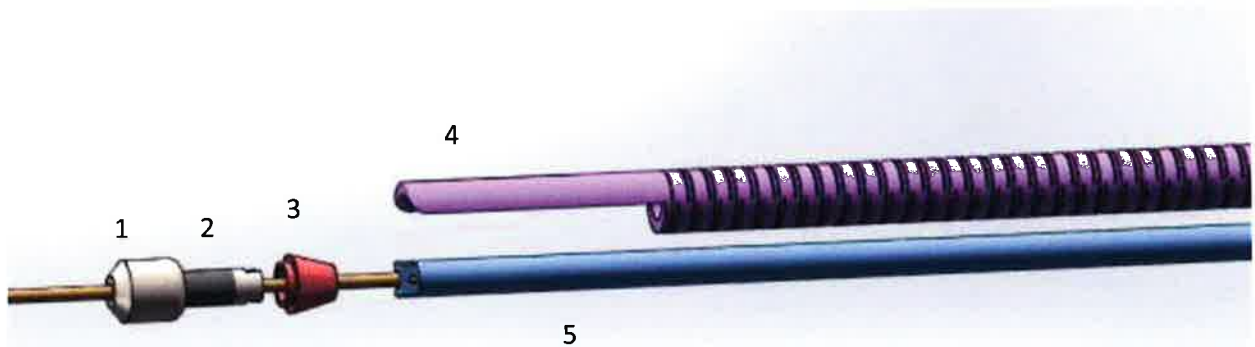


Figure 13: An exploded view of the distal portion of the directional reaming system is shown. Note the Aluminum grit blasted region (2) on the reamer cutting head (1) as well as the peek conical bearing with the added stainless steel shim (3) to separate the bearing from the cutting flutes of the reamer head. The flexible follower sleeve (4) is shown above the reamer shaft (5) which contains a spiral cut to induce flexibility (not shown).

D. Translating Reamer Prototype

In order to increase marketability of the directional reaming device and allow for the use of a 12mm diameter reamer head, the third prototype was constructed to be controlled by a ramp and plunger mechanism. The plunger is advanced along a partially enclosed stationary follower sleeve and is driven along a ramp at the distal end of the device near the reamer head. In order to minimize the effects of the dovetail connection on the amount of lateral reaming and maximize the distance the reamer head can eccentrically cut, the reamer head and shaft have been welded together. This allows for a smaller diameter reamer shaft to be used but will require a smaller guidewire. This in turn, may add a step to the operation by requiring the surgeon to change out the conventional 3mm stainless steel guidewire for a 2mm diameter stainless steel guidewire. However, the device will now allow the surgeon to attain a maximum of 4mm of lateral cutting into the inner diameter of the IM canal given a 2mm reamer head with a 4mm diameter reamer shaft.

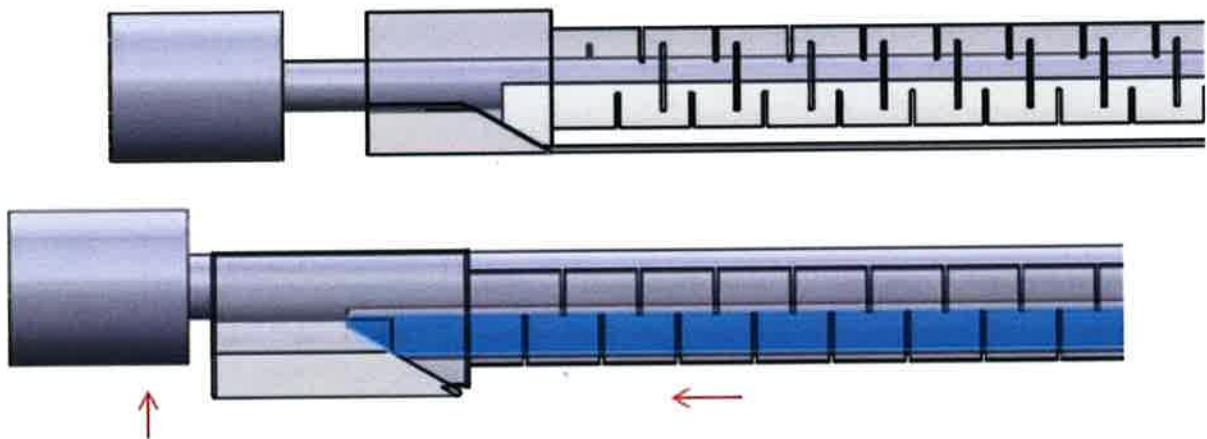


Figure 14: As the trigger is contracted towards the handle, the plunger is advanced up the saddle ramp. This causes the reamer shaft to be translated in one direction instead of deflecting the reamer head at an angle as in previous designs.

a. Plunger design

In order to translate the reamer head into an eccentric position, a peek plunger component was developed to slide along a ramp. The distal end of the plunger contains a 30° incline which induces the translation with a mating surface on the plug and connecting arm components. The material for the plunger was chosen to be peek to allow it to flex with anatomical curvature during operation. The plunger is driven proximally by a cylindrical pin feature which rests in a pair of slots on the trigger flanges. As the trigger is rotated about a point inferior to the flanges, the slots drive the plunger distally causing the inclined surface near the reamer head to travel up the ramp. A hard stop built with additional supporting volume was placed 10mm from the center of the cylindrical and extends 20mm along the length of the plunger. The additional material volume provides an enclosure for a locking ratchet tooth that in future iterations of the device will allow the surgeon to orient the length the plunger has traveled with respect to the distance the trigger has been contracted. The top surface of the plunger is rounded to steady the sleeve and reamer shaft as they rotate during operation. See **Figure 15** below for an illustration of the plunger concept.

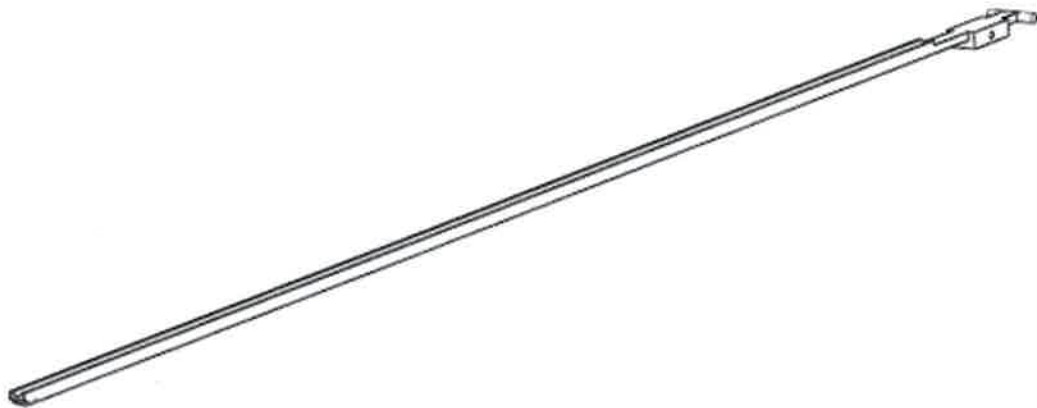


Figure 15: The distal end of the plunger contains a 30° incline to mate with the plug at the distal end of the device. The cylindrical feature on the proximal end rests within the trigger flange slots and allows the plunger to be translated forward as the trigger is contracted towards the grip. The rectangular region near the horizontal driving pin is the hard stop feature containing the cavity for the locking ratchet tooth.

b. Follower sleeve (Tube) and Plug Design

The follower sleeve for this iteration of the prototype is designed to have a similar bending stiffness to the previous model by having quadrant cuts the same distance apart as previous models. However, it differs in that the bottom of the sleeve is open to allow the plunger to create a rounded and flush surface prior to the plunger being advanced by the trigger. The objective is to ease the insertion of the reaming system into the IM canal while maintaining flexibility to match the curvature of the anatomy. In addition to the open bottom, this model of follower sleeve also contains a fluted opening from the connection at the plug for a distance of 36.6mm. As the plunger advances up the ramp, the fluted surface will act as a smooth surface for the reamer shaft surrounded by a peek jacket to rest against. At the distal end of the follower sleeve, a rigid plug is welded to support the reamer shaft. The plug contains the inclined surface to mate with the peek plunger. It also contains a flat surface to support the plunger at full displacement (translation). See **Figure 16** for illustrations of the follower sleeve and plug.



Figure 16: Shown above is the stainless steel plug and follower sleeve assembly.

c. Body Design

The body of the device has also been updated to be more ergonomic while giving the operator more control of the device during deflected reaming. It is also meant to be similar in appearance and

usability to reamer drivers to maintain a sense of familiarity with the device. Only the functional parts of the device related to directional reaming were made for the last cadaver study which will be completed the second week of May 2017. Unlike the previous versions of the directional reamer system, the translational prototype is enclosed to protect the safety latch and bearing assembly used to support the rotating reamer shaft. The trigger has also been improved by adding curved slots with a 9.2mm radius in the top flanges of the trigger to lessen the force necessary to drive the plunger forward. The trigger also contains a slot at the bottom to catch a spring loaded trigger lock which will immobilize the reamer head in an eccentric cutting position.

Two additional safety features are built into this design and meant to prevent inadvertent movement of the reamer head by the surgeon. First, instead of a continuous trigger motion to advance the plunger, a ratcheting system (6, 11, and 12 in **Figure 17**) was installed to aid the operator in indexing the amount of eccentric cutting by the reamer head. The ratchet can be disengaged by rotating the lever located in front of the trigger and just below the follower sleeve. The reamer shaft and plastic sleeve are held within the body by two rotating thrust bearing assemblies as shown in **Figure 17**. The reamer shaft and plastic sleeve are captured in a stainless steel bearing sleeve with a collet feature at the proximal end which will be chucked into the reamer driver.

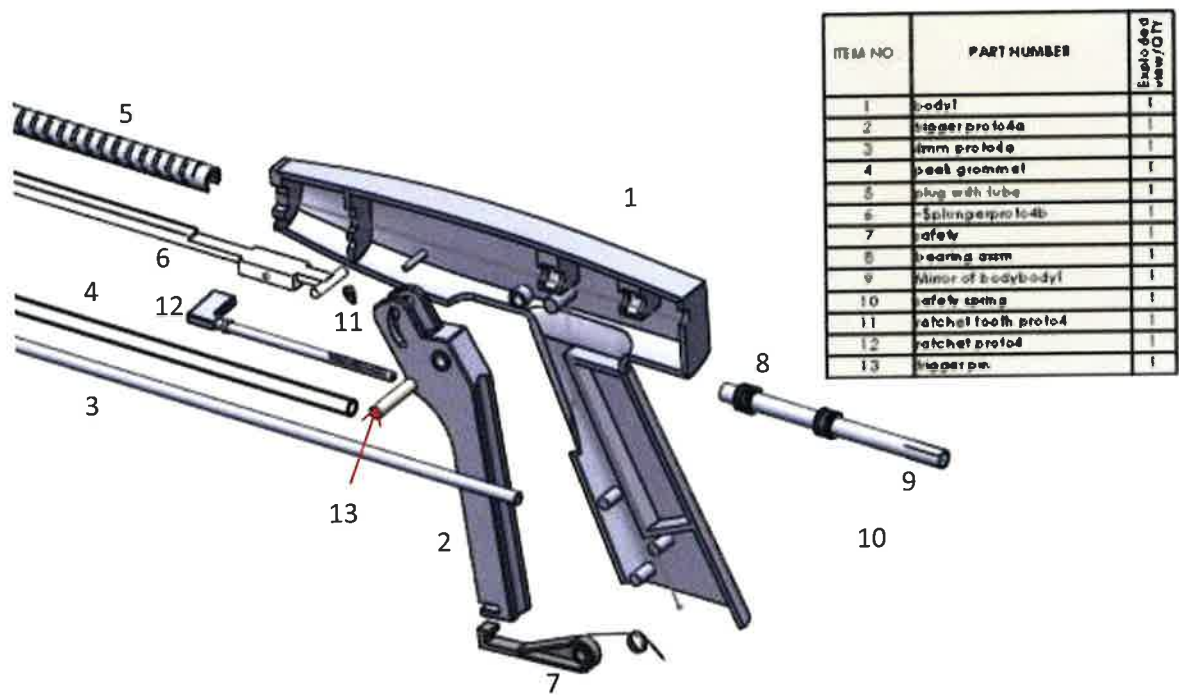


Figure 17: The proximal components of the directional reamer assembly are shown above. The mating shroud, trigger spring, and ratchet spring, and ball bearings have been omitted for visual clarity.

III. Materials and Methods

The prototypes were qualified first using a dry experiment then a cadaver study if favorable results were obtained. The first experiment involved a parallel plate fixture and was completed at the

manufacturing facility Devicix, LLC. This experiment involved laterally deflecting the reamer head into a planar MDF board to observe the depth of cut. The second prototype yielded favorable results in the dry testing and advanced to the cadaver study outlined in subsequent sections.

A. First Prototype (12mm Conical Insert)

- Test Fixture
 - 30cm Square Plate of Acrylic
 - 30cm Square Plate of MDF Board 1.9cm thick, 61cmX61cm
 - Steel Base Plate
- Concept Prototype Bearing
- Concept Prototype Follower Sleeve
- 3mm Diameter x 46cm 316 SS Rod (Guidewire)
- Stryker Reamer Shaft (0227-3000S)
- Stryker 12mm Bixcut Modular Head (0226-3120)
- Stryker Grommet (3212-0-210)
- Delta Drill Press (17-950L)
- Table Stand with Clamp
- Quick-Grip Clamp
- Clamp
- Calipers
- Video Camera with Tripod

a. Devicix Experiment 1

The first prototype containing the dove tail displacement insert and follower sleeve was evaluated on the depth of cut and lateral reaming capability in three trials with three different parallel plate positions. Prior to observing the cutting behavior in the fixture, material wear of the peek/stainless steel interface and assembly movement was evaluated in open air. The flexible shaft was chucked into a cannulated drill press in a vertical position with the follower sleeve clamped to a ring stand concentrically to the flexible shaft and guidewire (See **Figure 18**). The guidewire was allowed to rest on a table top 15cm below the assembly. The drill press was set to 250rpm to replicate the speed of most surgical drivers which range from an operational 250-300rpm. The drill press was retracted to cause the

reamer shaft containing the conical insert to engage the clamped follower sleeve and induce lateral deflection. The assembly was visually inspected for wear and structural damage; however no wear on either of the combinations of peek/stainless steel was present. Only a minor discoloration was present which could be wiped off and was likely due to manufacturing impurities.

In the first trial, the peek conical insert and stainless steel follower sleeve underwent three tests of deflected reaming. The deflection system was assembled and lowered between the MDF board and acrylic plates until the point just before the engagement of the follower sleeve with the conical insert. Once the assembly was in position and zeroed, the follower sleeve was clamped to the MDF board. The drill press was again activated to 250rpm and retracted to create contact between the stainless steel follower sleeve and peek conical insert. See **Figure 18** for the test setup of trials 1 and 2. The second trial replicated trial one using the stainless steel conical insert and peek follower sleeve. The reaming assembly was lowered between the plates and the drill press depth was again zeroed. Each test within trial two was completed according to the respective plate positions. The third trial utilized the stainless steel conical insert and the stainless steel follower sleeve to observe the interaction between the like materials as a bearing interface during deflected reaming. Trial three was only completed in position 3. Due to results similar to the first two trials, only one test was completed in trial three.

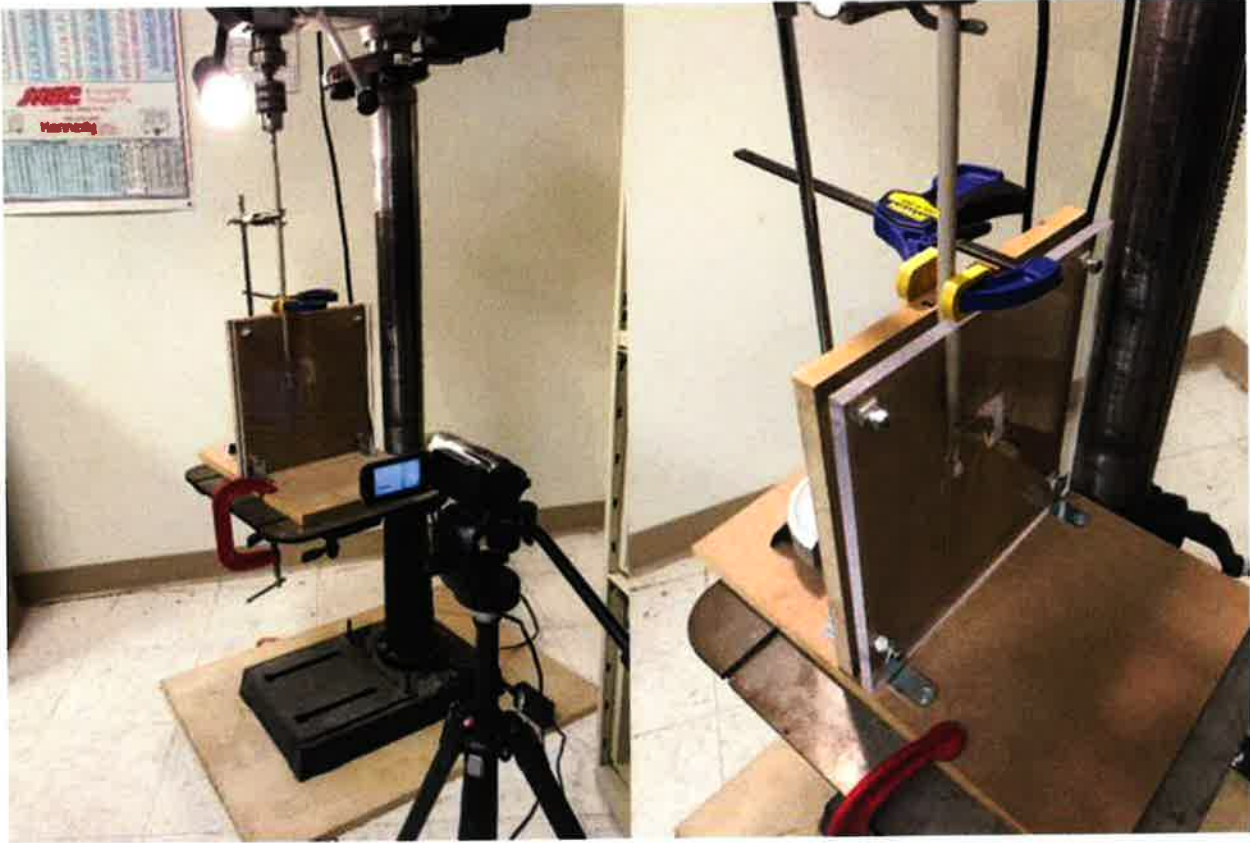


Figure 18: The test setup for the three trials is shown above. The image on the right shows the position of the reamer system between the plates with the follower sleeve clamped to the MDF board. In this figure, trial two containing the peek follower sleeve and stainless steel conical insert is shown in the fixture.

B. Second Prototype (14mm Conical Bearing)

a. Devicix Experiment 2

The first round of experimentation for the second prototype was completed at Devicix, LLC in a manner similar to the first prototype. However, in addition to the parallel plate test, trials involving foam femurs were included to replicate the curvature of a biological adult femur. The objective of this set of experiments was to evaluate the proposed reamer head deflection system in achieving a minimum of 3mm of lateral reaming within the parallel plate setup as well as the foam femur. This set of experiments included one trial using the parallel plate fixture and two trials involving sawbone (foam model) femurs (1130-27).

Materials:

- Flexible Follower Sleeve
- Modified 14mm Reamer Head with Peek Displacement Bearing
- Follower Sleeve Handle
- Parallel Plate Test Fixture
- Sawbones (1130-27) - quantity 2
- 3mm diameter x 1.5ft 316 SS rod (guidewire)
- Stryker reamer shaft (0227-3000S)
- Stryker 14mm Bixcut modular head (0226-3140)
- Stryker grommet (3212-0-210)
- Delta Drill Press (17-950L)
- Rigid Hand drill, ½" chuck (Model R86008) [2 speed: 0-450, 0-1650 RPM]
- Table stand with clamp
- Table vise
- Quick-grip clamp
- Clamp
- Caliper
- Video Camera with tripod

Procedure (Parallel Plate):

First, the prototype was assembled without being attached to a driving system to ensure no component interference would occur during operation. The flexible follower sleeve was placed concentrically over the Stryker flexible shaft, and the modified reamer head was attached to the flexible shaft using the dovetailed connection at the distal end of the flexible shaft. The handle was added over the follower sleeve and was tightened using a wrench to the proximal end of the sleeve using the two set screws in the handle. The handle was aligned in the direction opposite of the deflection of the reamer head. Once the prototype was assembled, the flexible shaft was marked for the point at which the follower sleeve fully engaged the displacement bearing. This allowed the user to observe when the follower sleeve had obtained possible maximum deflection as well as to prevent the user from advancing the follower sleeve into the cutting flutes of the reamer head.

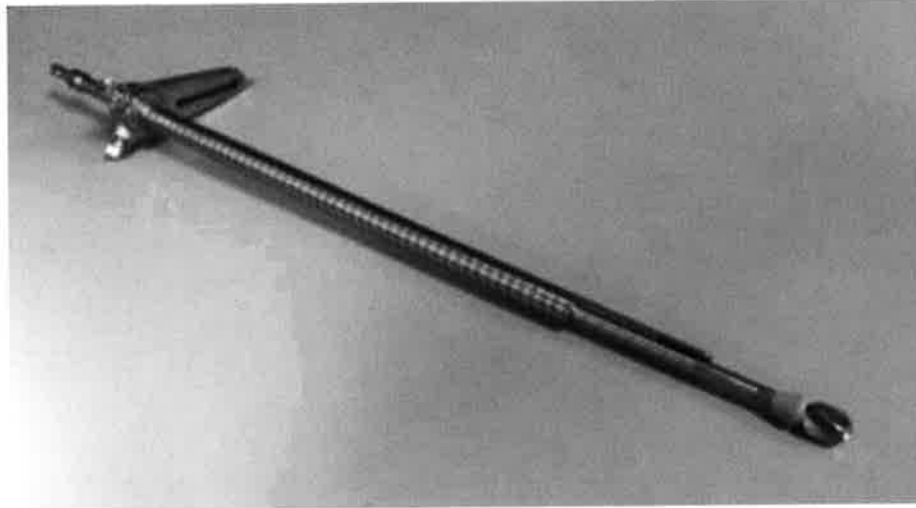


Figure 19: The completed prototype is shown above. Note: this system is cannulated for inclusion of a guidewire (not present).

The parallel plate fixture was placed under a drill press for the first round of tests. The video camera was placed on a tripod facing the test fixture with the viewing window directed between the parallel plates. The drill press was set to operate at 250rpm since the standard operating speed of a surgical driver ranges between 250-300rpm. Next, the reamer assembly was placed between the parallel plates of the test fixture then raised to be chucked into the drill press. Once the assembly was located vertically without interference between the parallel plates, the proximal end of the flexible shaft was chucked into the drill press. This location between the plates was labeled as *Position A* on the top surface of the MDF plate. The fixture was clamped onto the base plate of the drill press. A ring stand/table clamp was then positioned laterally to the MDF plate and clamped onto the base plate. The table clamp was used to stabilize the follower sleeve and maintain the alignment of the follower sleeve tongue opening towards the MDF plate. The spacing between the parallel plates was measured at each corner and at the center of the top (all measurements 14.00mm). The follower sleeve was also clamped to the MDF plate to immobilize the follower sleeve during testing. It is important to note that the follower sleeve was immobilized in a position not contacting the displacement bearing. At this location, the drill press was set to measure a depth of 0.0mm.

Procedure (Sawbones):

A sawbone (foam model of a bone) was positioned in a vice with the distal end (medial and lateral femoral condyles) facing upward. A quick-grip clamp was used as a second location of anchoring to prevent axial movement or pivoting. Next, the foam plug located between the femoral condyles was removed and 3mm guidewire was inserted into the IM canal. The follower sleeve was removed from the directional reaming assembly. The assembly was then chucked into a power drill and inserted over the guidewire. The power drill was set to a maximum speed of 450rpm. The 9mm IM canal was then reamed to 14mm for a length of 12.7cm using the modified head designed by the university team and Devicix, LLC. The reaming assembly was removed from the sawbone and guidewire, and the reamer head was removed. The follower sleeve was added to the assembly by sliding it over the flexible shaft starting from the distal end. The reamer head was replaced and the assembly was again inserted over the guidewire. Just prior to entering the IM canal, the drill trigger was depressed half way to cause the reamer to rotate at approximately 250rpm (representative of surgical use). Using the handle attached to the follower sleeve, the sleeve was kept from engaging the displacement bearing as the assembly was advanced along the canal. Once the reamer head had reamed a distance of approximately 10cm, the follower sleeve was partially deployed to initiate deflected reaming and allow space within the IM canal for the displacement bearing and flexible shaft to be deflected. The follower sleeve was then retracted and advanced to fully engage the displacement bearing.

In the second sawbone trial, the epiphyses were removed from the second femur in order to ensure that the representative cortical bone was reamed during testing. In the previous trial, deflected cutting was performed before the reamer head reached the cortical shaft of the sawbone. With both epiphyses removed, the diaphysis was then placed in a table vice in the same orientation as the sawbone in the previous trial (distal end up). A quick-grip clamp was again used to immobilize the sawbone. The guidewire was placed within the canal and allowed to rest on the axle of the vice. The reamer head was

removed to allow for the removal of the follower sleeve. The modified 14mm reamer head was replaced, and the IM canal was reamed to 14mm. Once the canal was reamed, the follower sleeve was replaced in the assembly. Again, prior to the assembly entering the IM canal, the drill trigger was depressed half way to rotate the reamer head at an approximate 250rpm. The follower sleeve was kept from engaging the displacement bearing by use of the handle attached at the proximal end of the follower sleeve. The handle was also kept in the same position while the reaming assembly was advanced through the canal. Once the reamer head reached 50% of the length of the sawbone, the follower sleeve was advanced over the conical insert. As with the previous trial, the follower sleeve was partially engaged and retracted prior to creating full displacement of the bearing. The assembly was then advanced as the follower sleeve was fully engaged to create the maximum amount of deflection of the bearing without impinging on the inner wall of the canal. The handle was used to advance the follower sleeve and was kept in alignment throughout the reaming process.



Figure 20: Devicix saw bone test is pictured above.



Figure 21: (Left) The second sawbones trial is shown above. The epiphyses were removed for this round of testing to allow the operator to more easily gage the distance of the reamer head down the IM canal of the sawbone. (Middle) A close-up view of the deflected cut is shown in the coronal plane. The sawbone experienced minor cracking during the cutting along the coronal plane to expose the deflected cut. This had no effect on the measured results of the experiment. (Right) The depth of maximum deflection was 5.74mm. No walking or otherwise detrimental effects of deflecting the reamer head are evident from the results meaning a successful experiment. From these results, the directional reaming system was proposed to be tested in a cadaver study.

b. Cadaver Experiment

Introduction:

Due to the success of the 14mm design in the sawbone trials completed at Devicix, a cadaver experiment was conducted to observe the directional reaming capability in human tissue. The objective of this study was to quantify the directional reaming capability of the proposed design. The system must achieve a minimum of 3mm of lateral reamer head displacement during reaming. This experiment took place in the University of Louisville's Fresh Tissue Dissection laboratory using a female cadaveric femur. The donor was an 86 year old female who expired due to end stage renal disease. The renal disease was not identified as a factor affecting the results of the experiment. In the first round, the intramedullary canal was shaped simply advancing the follower sleeve over the reamer head followed by circumferentially reaming by rotating the assembly axially during operation. Cutting location and depth estimates were obtained using an OEC 9800 neurovascular C-arm. After testing, the bone was opened, and the depths of the cuts were measured using calipers.

The study consisted of two rounds of testing with two trials completed in the first round and two trials completed in the second round. The first trial included simply applying the follower sleeve to the displacement bearing to achieve a point of 3mm lateral displacement. The second trial included applying the follower sleeve then moving the reaming assembly to ream a longitudinal trough along one side of the IM canal.

Materials:

- Stryker Bixcut reamer head set
- Video camera
- Modified 14mm reamer head containing peak displacement bearing
- Stainless steel flexible follower sleeve
- Stryker 8mm diameter dovetailed flexible reamer shaft (480mm)
- Reamer driving assembly
 - Standard power drill
 - Cannulated surgical driver
- Bone drilling assembly (surgical driver and drill components)
- Cadaveric femurs (2)
- Lab table
- Operating tray (preferably with drain or irrigation)
- Orthopaedic table clamp
- Awl
- Guidewire insertion handle
- Reamer irrigator/aspirator if available
- OEC 9800 Neurovascular C-Arm
- Bowl or rinse water and cleaning syringe
- Sawbones Oscillating Saw - Pacific Research Labs, INC.

Procedure (Round 1):

In order to extend the time of the cadaveric femurs' usability, all residual soft tissue was removed from the outside of the bones. Next, the femurs were returned to the freezer for two weeks while parts were obtained to conduct the experiment. Once the parts had been received by the student and project director, the femurs were allowed to thaw. One femur was used for the two rounds of

experimentation, and the second femur was returned to the cooler and was eventually acquired by a separate team.

First, the femur was immobilized in the table clamp in an orientation representative of an antegrade femoral intramedullary operation. This orientation was chosen due to its overall success in minimizing malunions and comminution during operation[28]. The proposed directional reaming device should perform in a successful manner whether operation is performed in an antegrade or retrograde fashion, but future experimentation is necessary to validate the system's performance in a retrograde operation. An awl and a 10mm drill bit were used to create clean access to the IM canal through the piriformis fossa. The guidewire was then inserted into the canal with care taken to ensure it was seated firmly in the distal epiphysis. It may be necessary to tap the guidewire handle stabilizing the wire in place to prevent unwanted movement during the reaming process. Once the guidewire was in place, the Stryker 12mm reaming system using a cannulated Stryker driver on the low power setting (250-300rpm) was used to ream over the guidewire into the IM canal until the distal epiphysis was reached. Next, the 12mm reamer head was exchanged for the modified 14mm reamer head containing the peek displacement bearing since another 14mm reamer head was unavailable. The IM canal was then reamed to a 14mm diameter. This iteration of reaming required slower progression through the canal in order to prevent excess medullary content buildup from the hindrance of the displacement bearing. The reaming assembly was removed, but the guidewire was left positioned in the canal. The handle was then tightened to the flexible follower sleeve in line with the direction the reamer head will be deflected. Following the expansion of the canal to 14mm, the modified reamer head was removed and the follower sleeve was inserted over the flexible shaft followed by reattachment of the modified reamer head. The follower sleeve was then aligned next to the femur to mark the follower sleeve for locations corresponding to the point of reamer head deflection within the IM canal. The locations were marked in percentage of length of the diaphysis as follows: 25%, 40%, and 50%. Two marks were made on the

flexible shaft signifying the point just before the follower sleeve engaged the displacement bearing and the point of maximum deflection (full engagement of the follower sleeve).

Once the marks were placed on the respective shafts, the reaming assembly was placed concentrically over the guidewire and inserted into the canal. Care was taken to ensure that the follower sleeve did not engage the displacement bearing and that the handle maintained alignment with the direction of the reamer head deflection. The driver was activated and the reaming assembly was advanced in a stepwise fashion to the 50% mark as is standard practice in the reaming process[29]. Due to the similar diameters of the follower sleeve and reamer head as well as the length of the rigid tongue of the follower sleeve, it was difficult to advance the follower sleeve through the IM canal with the reamer shaft. This made it necessary to rotate the follower sleeve from the handle to reach the correct location. Once the 50% mark on the follower sleeve was at the point of entering the femur, the handle was aligned vertically and above the flexible shaft in order to maintain a constant direction deflected cutting towards the anterior cortex of the IM canal. The follower sleeve was advanced slowly until the point marked on the flexible shaft was reached signifying the point just before the follower sleeve tongue engaged the displacement bearing. The follower sleeve was advanced and retracted three times to ensure a clean cut at the location; then the reaming assembly was removed (while activated) from the femur along with the guidewire. Upon removal of the reaming assembly, the reamer head and shaft was cleaned using a syringe filled with water to clear reamed debris. A metal wire was wound around the location of the displaced cut to assist the team in identifying the location of the cut on X-ray.

Once the reamer was removed, release the femur from the table clamp and allow the residual intramedullary contents to drain onto the table tray. The femur was then transferred to an adjoining lab where an OEC 9800 Neurovascular C-Arm fluoroscopic x-ray machine is stationed. The x-ray emission component was connected to the viewing station and the C-Arm was activated along with a USB storage converter to save the digital fluoroscopic images. In order to capture each x-ray, the *Image Capture*

button was pressed after each x-ray is taken. The x-rays were used to estimate the location and quality of the deflected cutting at each level within the IM canal. The femur was placed on a tray within the C-Arm while an image was taken in the coronal plane. Next the femur was rotated 90° clockwise to capture the sagittal view. The femur was returned to the table clamp in the same position as the previous round of testing. The guidewire was inserted into the original position within the IM canal and the reaming assembly was placed over the guidewire. The reamer was inserted in the same manner as before until the 40% mark was visible just outside of the opening made at the piriformis fossa. The steps for creating a deflected cut in the inner wall of the IM canal were repeated by advancing the follower sleeve to the mark on the flexible shaft representing the point just before the sleeve contacted the displacement bearing. Next, the follower sleeve was advanced to the engagement mark and retracted to the disengagement mark three times to ensure any eccentrically reamed debris was cleared before removal of the reamer. The reaming assembly including the guidewire was removed from the IM canal. Following this round of testing, the exterior of the femur and reaming assembly were cleared of medullary contents using paper towels and a syringe of water. Using the 40% mark on the follower sleeve as a guide, the metal wire was placed at the 40% location on the femur to assist in locating the cuts under x-ray. The femur was released from the table clamp; and the medullary content was drained by positioning the bone vertically with the IM canal portal facing the operating tray. Afterwards, fluoroscopic x-rays of the coronal and sagittal planes of the femur were again taken using the C-Arm. Once coronal and sagittal views had been captured, the images were stored individually on the external USB device and the bone was returned to the table clamp in the same orientation as the previous rounds of testing.

The guidewire and reaming assembly were reinserted into the canal in the same location, and a deflected cut was created at 25% of the length of the canal in a similar manner to the previous two trials. However instead of simply moving the follower sleeve forward to the bearing engagement mark, the

reamer was retracted halfway between the pre-engagement mark and the fully engaged mark on the flexible shaft. Next, the reamer was advanced to the disengaged position. This action prevented impingement of the flexible shaft and displacement cone on the wall of the IM canal during deflection. The entire assembly was advanced 1cm while moving the follower sleeve to the engaged position marked on the reamer shaft. The reaming assembly and guidewire were removed and cleaned with water, and the femur was drained of reamed medullary contents. When the reamer was removed from the canal, wear was noticed on the peek bearing; however, this seemed to be negligible and caused no identifiable effect on the performance of the deflection of the reamer cutting head. The femur was placed within the C-arm to capture coronal and sagittal views of the deflected cut. The *Save Image* button was pressed on the USB storage after each x-ray.

The femur was returned to the table clamp and the reamer assembly (including the guidewire) was replaced in the IM canal for a final test. The assembly was again advanced to the 50% mark on the follower sleeve shaft with the handle guiding the follower sleeve tongue to create an anterior cut. However, the handle orientation was not critical in this test since a rotational cut along the inner circumference of the IM canal will be performed. The follower sleeve was advanced to the pre-engagement mark on the flexible shaft. The reamer was activated; then the follower sleeve was engaged. The follower sleeve handle was rotated axially 360° three times while the sleeve was engaged against the displacement bearing in order to create a clean cut. Once the reamer was removed and again cleaned, the femur was released from the clamp and drained of intramedullary contents by rotating the femur longitudinally so that the portal accessing the IM canal faced the operating tray. X-rays were again taken; one in the coronal and one in the sagittal plane. The student and director noticed that a substantial amount of medullary content was present within the section of the circumferential cut (**Appendix E: Figure 42**). The femur was replaced in the table clamp and the reaming assembly was used

to clear the debris without deflecting the reamer head. Secondary x-rays (**Figure 32**) of the circumferential cut revealed a more defined cut without the presence of the reamed debris.

Once all trials had been completed, the femur was taken to the university orthopaedic laboratory for analysis of the cuts made. The femur was placed in a table vice in the supine position in the same manner as in the table clamp during the reaming operations. Next, a hack saw was used to make a cut across the intertrochanteric line and superior to the lesser trochanter to the midline of the femur. A cut at a 60° angle was made at 60% of the length of the femur to the axial midline of the femur. In order to cut along the diaphysis of the femur along the midline, four holes were drilled 2mm above the base of the 60° cut to allow room for the hack saw blade. The hacksaw blade was inserted to cut along the diaphysis towards the first cut made at the intertrochanteric line. The hacksaw handle was then attached to the blade with the frame resting against the anterior of the femur. The saw was advanced until the blade reached the axial midline of the diaphysis. The handle was then removed from the blade and reattached with the frame resting on the posterior of the femoral shaft. The hacksaw was advanced until the blade passed the axial midline of the diaphysis. The handle was removed and returned to the anterior side of the femur. This process was repeated until the perpendicular cut made across the intertrochanteric line was reached allowing for removal of the cut segment of bone. The canal was washed with warm water and paper towels until the bone shavings had been removed and the canal was cleared to cleanly show the IM wall. The locations of the directional reaming were then observed visually and quantified using Mitutoyo digital calipers. Due to the nonlinear cut made by alternating the hacksaw on the anterior and posterior sides of the femur, it was unclear where the circumferential cut may have been completed.

Procedure: (Round 2)

The bench top was draped and the drainage pipe was firmly connected to the floor drain under the worktable. The femur was immobilized using the table clamp and the wires holding the previously cut fragment onto the bone were removed along with the cut fragments themselves. The guidewire was threaded into the IM canal through the hole created during the first round of testing and firmly seated into the distal diaphysis. The reaming assembly (with the modified 14mm cutting head) was chucked into a cannulated surgical driver and placed over the guidewire. The canal was then reamed to clean any debris that may have been present in the IM canal. This ensured that a minimal amount of reamed debris would be present to cause the system to bind during testing. The reamer was activated and driven to the end of the IM canal in the distal diaphysis. Next, the reamer was removed from the IM canal, the modified reamer head was removed from the shaft and the reamed tissue was washed from the assembly using a syringe and water with paper towels. The follower sleeve with the handle was inserted over the flexible shaft once the reaming components had been cleaned. The handle was aligned to correspond to the direction of deflected cutting. The directional reaming assembly was then inserted into the IM canal through the portal made in the previous round and advanced until the bearing's proximal edge reached the distal edge of the exposed region of the IM canal. The camera was activated to capture the location of the reaming assembly and record the directional capability of the bearing. Since the shaft and proximal end of the displacement bearing were exposed in this trial, the reamer assembly was retracted in the same manner as the first parallel plate experiment because the IM canal wall was not present to cause impingement of the shaft and bearing deflection. A point of displaced cut was created at this location by advancing and retracting the reamer three times. Next the reaming assembly was removed from the IM canal and cleared of any tissue using water and paper towels. Additional wear was noticed on the peek bearing which would decrease the amount of deflection possible. Due to the curvature of the femur and the exposed region of the IM canal, a bending moment towards the anterior plane was created at the deflected reaming location. Since the reamer head was deflected medially, this moment was not expected to affect the results.

For the second trial, the reaming assembly was inserted through the exposed portion of the diaphysis wall and into the remainder of the distal IM canal. This eliminated the moment caused by the curvature of the femur and allowed for a more linear approach of the reamer head to the cutting location. The reamer head was advanced into the canal 10mm past the first trial and the steps for deflected reaming were repeated on the lateral wall of the IM canal. It was noticed that while reaming, the follower sleeve was advanced too far and came into contact with the cutting flutes of the reamer head. After the sleeve had been advanced three times over the bearing, the assembly was removed and cleaned of reamed tissue. Substantial wear was observed on the bearing as well as a circumferential line near the base of the bearing where the edge of the bevel in the follower sleeve tongue came into contact with the bearing when the follower sleeve was advanced too far. Minimal damage to the follower sleeve was also present at the location of cutting flute contact. No visible damage was present on the reamer head. An oscillating saw was used to expose the locations of deflected reaming by cutting a quarter of the diaphysis away as shown in **Figure 22**.

C. Third Prototype (Translating System)

Sawbone Experiment

Introduction:

The sawbones experiment was conducted at the University of Louisville's orthopaedic research laboratory. The criteria for success remained the same for this prototype as the previous two in order to bring it to a cadaver study. The parallel plate setup was no longer needed with the implementation of the foam bone models and was subsequently bypassed. Three trials will be conducted along the foam femur's intramedullary canal at 20%, 30%, and 40% of the length of the canal. From these cuts the depth of directional reaming will be measured using calipers. Due to manufacturing limitations, a 12.5mm reamer head and plug were constructed for the completion of this prototype.

Materials:

- 12mm drill bit
- Table Vice
- Parallel Plate Test Fixture
- Sawbones (1130-27) - quantity 2
- Rigid Hand Drill, ½" chuck (Model R86008) [2 speed: 0-450, 0-1650 RPM]
- Quick-grip clamp
- Clamp
- Calipers (Mitutoyo CD-6"CS)
- Hollow 4mm Reamer Shaft and 12.5mm Reamer Head
- Delrin Plunger
- Stainless Steel Plug (12.5mm) with Attachment Arms
- Line Level
- One cancellous Bone Foam Model
- Two Cortical Bone Foam Models

Procedure:

Access to the foam femur's proximal intramedullary canal was obtained using the Rigid power drill and the 12mm drill bit. The Delrin plunger was aligned within the stainless steel plug and the reamer shaft was seated in the plug and over the plunger. The reamer head was located 1.5mm from the distal surface of the plug. The assembly was then held next to the foam femur, and depth marks were placed on the attachment arms to indicate the relative cutting depth when the assembly was placed into the IM canal. The plunger was also marked for locations indicating neutral position and complete advancement into the plug. Next, the drill bit was removed, and the hollow 4mm reamer shaft and head were chucked into the drill. The drill was then activated to approximately 250rpm, and the reaming assembly was inserted into the IM canal to the 25% mark on the attachment arms with the opening of the plug oriented towards the medial side of the femur. Once the 25% mark was reached, the plunger was advanced until full displacement of the reamer head was achieved. The plunger was then retracted and the reaming assembly was withdrawn from the canal. The drill was then deactivated. The cutting flutes of the reamer head were cleared of foam shavings, and the assembly was returned to the outside edge of the bone. The drill was reactivated, and the assembly was inserted to the 30% mark

inside the IM canal. The plunger was advanced to full capacity and retracted. Since no noticeable eccentric depth of cut was observed upon removal of the reaming assembly, reaming on the lateral side of the IM canal was conducted at the 30% length mark. During this trial, the adhesive holding the reamer head onto the reamer shaft failed causing complete dislocation of the head from the reamer shaft. The assembly was removed from the canal with the reamer head removed separately. A second adhesive, a two part epoxy, was used to repair the reaming system. The sawbone was removed from the table vise, and the distal diaphysis was removed. The bone was opened along the sagittal plane to record the depth of cuts using the Mitutoyo calipers. The sawbone was cut perpendicular to the end of the sagittal cut allowed for the removal of the lateral cortical wall exposing both the 20% and 30% length cuts. After opening the IM canal, it was observed that the foam IM canal was 15.85mm in diameter. This allowed only 1.675mm of additional cortical wall removal with the designed system.

After allowing the two part epoxy to set over night, the prototype was again assembled for foam model testing. A second experiment using a rectangular 30 x 40 x 130mm foam model replicating cancellous bone was used. The 12mm drill bit and Rigid power drill were used to create a pilot hole for the reaming assembly. The drill bit was removed, and the directional reaming prototype was assembled. The reamer shaft was chucked into the power drill. The drill was activated to approximately 250rpm, and the assembly was inserted into the pilot hole in the foam model. The plunger was advanced causing full deflection followed by removal of the reaming assembly. The model was opened using a hacksaw in the same manner as with the foam femur to expose the eccentrically cut areas.

A rectangular cortical bone foam model of the same dimensions as the cancellous model was used for the next trial. The 12mm pilot hole was repeated for the model followed by insertion and activation of the prototype. During advancement of the plunger, the epoxy failed causing complete displacement of the reamer head from the shaft. The assembly was removed with the reamer head removed separately. The epoxy was filed from the external surface of the reamer head and shaft and

removed from the inner surface of the reamer head using a 3mm diameter drill bit. The reamer head was then welded to the shaft, and another rectangular cortical bone model was acquired. The pilot hole was again created in the same manner as with the previous trials, and the assembly was inserted. During deflected reaming, the 4mm diameter hollow reamer shaft failed in shear 16.3mm from the proximal edge of the weld. The prototype and distal reamer segment were removed from the model. it should be noted that the reamer head was too hot to touch upon immediate removal from the foam model, but the sheared segment of the shaft was not.

IV. Results

A. First Prototype (12mm Conical Insert)

Though this design yielded the necessary deflection when calculating the predicted movement of the reamer cutting head, the conical insert assembly failed to achieve the target 3mm minimum lateral deflection during testing. It was observed during preliminary testing that the added dovetail attachments contained too high of tolerance values and allowed a significant amount of reverse displacement to occur at the dovetail connections as the follower sleeve engaged the conical insert. It was also found that the guidewire caused substantial resistance to the reamer head deflection. From this observation, a proposed change in future operation procedures is to withdraw the guidewire proximally until only two to three centimeters of the guidewire extends from the distal end of the reamer head. In an effort to eliminate the effects of the dovetail tolerance issue, the decision was made to replace the dovetail insert with a conical bearing to fit over the cylindrical section of the reamer head. In order to induce sufficient displacement, a 14mm reamer head was suggested for development.

TABLE 1: CUTTING DEPTHS OF FIRST PROTOTYPE

Position	Cut Depth
1	0.98mm
2	2.18mm
3	1.02mm



Figure 22: All parts were again visually inspected for wear and structural damage. Scuff marks and discoloration can be seen on the inner diameters of the peek and stainless steel follower sleeve tongues. Although not clearly visible from the available pictures, slight discoloration was also present on the peek conical bearing displayed on the right.

B. Second Prototype (14mm Conical Bearing)

Results (Parallel Plate Fixture):

The maximum depth of deflected reaming reached from the parallel plate trials was 2.3mm. Therefore, this round of testing was considered a failure due to wall impingement of the bearing and possibly the flexible shaft. Since the drill press retracted the flexible shaft into engaging the follower sleeve tongue instead of advancing the follower sleeve, no material could be reamed prior to the lateral movement of the displacement bearing. The follower sleeve is intended to be advanced over the displacement bearing partially if needed, and allow space for the bearing to be displaced. The reaming assembly could then be advanced to that location, and the follower sleeve could be completely engaged over the bearing causing a full displacement of the reamer head.

During this round of experimentation, substantial wear and deformation was also noticed on the peek displacement bearing. The drill press rotated the reaming assembly continuously in the same location during experimentation causing pressure and subsequent friction between the bearing and plates as well as between the bearing and follower sleeve tongue. The amount of wear seen from this test is not expected to be present in clinical use since the reamers will not be run continuously but

instead in controlled cycles of activation to minimize heat buildup within the IM canal. The results of the parallel plate experiment may be observed in **Figure 23** below. In order to present a more clinically relevant result, the directional reaming system was tested in two rounds of experiments using sawbones. This experiment setup was meant to provide a closer representation to operation within a bone by providing a shallow curvature of the IM canal as well as two different layers of foam replicating different types of bone (cortical and cancellous).



Figure 23: Circled above is the location of deflection reaming using the 14mm reamer head. Only a depth of 2.3mm was achieved from this trial.

Results (Sawbones):

The first sawbone was cut along the coronal plane to expose the deflected cut. The reamer did not reach the representative cortical bone in this trial but was successful in creating an eccentric cut of 3.55mm. In the images below, the deflected cut may be seen on the right hand side of the exposed canal. Since the deflected cut was not completed on the representative cortical bone, the trial was repeated on the second sawbone in which both of the epiphyses were removed. This sawbone was also cut in the coronal plane to expose the deflected cut which was created midway down the diaphyseal shaft. The maximum deflection achieved from this trial was 5.74mm.

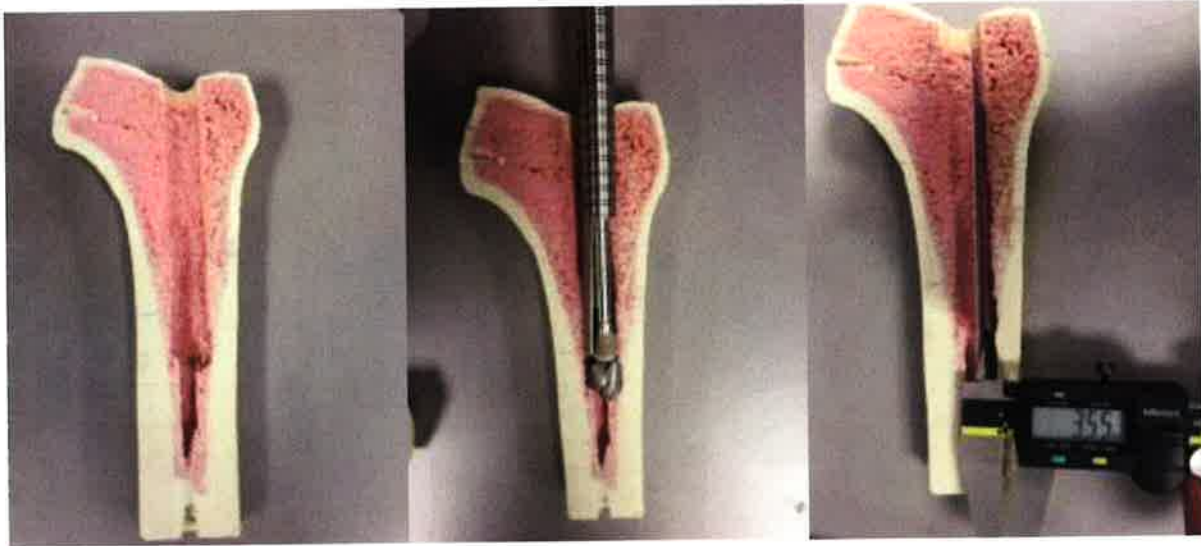


Figure 24: (Left) The first sawbones trial is shown above. The deflected cut did not reach the cortical shaft of the sawbone; however, a maximum depth of 3.55mm was achieved. (Middle) A representation of the reamer's deflected position is given within the site of the deflected cut. (Right) The method of measurement is shown above.



Figure 25: The modified reamer head on the left is unused and shows the amount of wear the reamer used in the sawbones experiment (right) sustained.

Conclusion (Sawbones):

The sawbones trials were successful in producing a deflected cut of at least 3mm. It is evident that attention must be given to the method of conducting a point deflection of the reamer head in order to achieve maximum displacement. Unlike in the parallel plate trials, the follower sleeve was able to be

advanced part of the way along the displacement bearing to allow room for bearing and shaft displacement as the reamer head was deflected. Unless the need is designed out of subsequent prototypes, this may be a technique which must be translated to the end user.

While the sawbones trials were successful in completing the objectives initially described, improvements may be made to the system to address certain usability issues. First, a more efficient method of advancing the follower sleeve is necessary. While the handle used in these experiments provided a robust means of adjusting the follower sleeve, it is recommended that a more ergonomic handle would allow greater control of the follower sleeve and add to the safety of the operation. Another improvement to the system that may be incorporated into the handle is an indexing system to control the amount of lateral deflection during reamer activation. This system may be implemented in a number of ways including a ratcheting system with an incremental set of deflection locations or an indicator along the follower sleeve only showing the operator the amount of deflection created. This method could allow for a continuous deflection up to the maximum deflection limit.

Results (Cadaver Study):

After the removal of the bone segment covering the locations of directional reaming, the depth of each directional cut was evaluated. Upon observation of the exposed intramedullary canal, the team realized the shape of the canal was likely irregularly shaped with a maximum diameter greater than 14mm in the direction of deflected reaming. This conclusion was drawn from the fact that medullary bone structure had remained intact along the inner wall of the canal corresponding to the linea aspera. A measureable amount of deflected reaming was accomplished at the 25% location. Only 1.66mm of lateral reaming was achieved at this location. Some wear of the peek bearing was observed after this trial; however, it appeared to be negligible (less than .25mm) and was not expected to affect deflection of the reamer head.

For the second round of testing, deflected reaming was completed on the medial and lateral walls of the IM canal to ensure a cleanly reamed area for directional cutting. The first trial on the medial wall yielded 1.04mm of deflection. The second trial did not yield any observable amount of deflection. The peek bearing sustained a total of .8mm of degradation to the maximum diameter owing to the lack of deflection in the second round of testing.

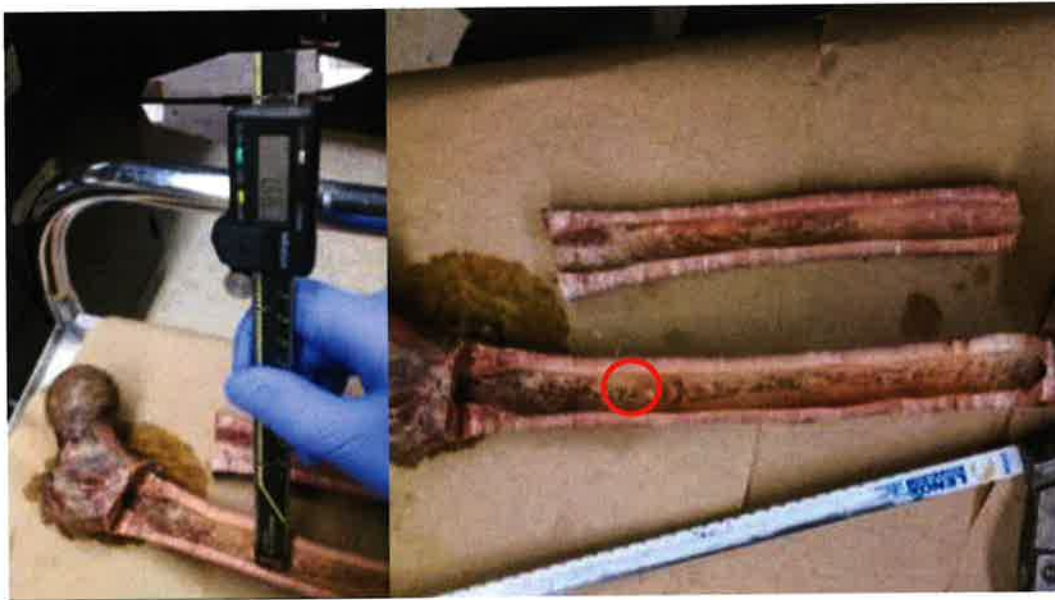


Figure 26: (Left) The maximum deflection achieved from the first round of cadaver testing was 1.66mm. (Right) The deflected cut is circled above. Upon removal of the anterior section of cortical bone, it was found that the anterior and posterior walls of the IM canal were irregularly shaped and did not present a smooth surface for easily observing a clean deflected cut into the IM canal wall. For this reason, the team performed the second round of testing on the medial and lateral walls of the canal.



Figure 27: (Left) The second round of deflected reaming took place in the circled area shown above. The cut was made in the distal region of the femoral diaphysis on the medial wall. The deflected cut was exposed using an oscillating bone saw to create a quarter length cut along the diaphysis. (Right) A close up image of the deflected cut is shown in the darker shaded side of the image. The deflected cut is called out in red.



Figure 28: The maximum amount of deflection at this location was found to be 1.04mm. Thus, this model of a directional reaming device did not achieve the qualifying criterion of 3mm of lateral deflection as dictated in the experiment objectives. The main contributing factor to this result is bearing wear due to the friction between the stainless steel follower sleeve and the peek bearing. A possible solution to this issue is reversing the materials of the follower sleeve and bearing. However, a more practical solution may be found with the next iteration of the directional reaming system involving a canal plug and reamer shaft saddle.



Figure 29: The peek bearing sustained substantial wear throughout the two rounds of testing (.8mm of material lost). It is suggested that if modifications to this design are performed, reversing the material of the bearing and follower sleeve may be more advantageous to reducing the amount of wear to the components.

Conclusion (Cadavers):

From the studies completed, it has been concluded that while directional reaming with a 14mm reamer head is possible, it is not practical to pursue this design for clinical use. The conical bearing design has several flaws that have become evident through testing. First, a higher strength material is

necessary to maintain a maximum diameter of the bearing to prevent wear from contact with the follower sleeve. It may be advantageous to switch the materials of the follower sleeve and bearing since peek is already flexible and would not require the cutting process necessary to make the stainless steel sleeve flexible. A stainless steel bearing would also sustain less wear than a peek bearing if used in conjunction with a peek follower sleeve. The stainless steel sleeve also contained a tongue that was too long to accommodate the curvature of the femur. This caused difficulty in advancing the sleeve along the canal and damaged the IM canal in some areas. For this reason, future tests using this design should include a shorter follower sleeve tongue that still allows for a reasonable amount of shaft flexibility. Other than the amount of wear sustained by the peek bearing, another limitation of this study was the effect time had on the osseous tissue. The femur was kept in an industrial cooler between rounds of testing for one month. However, since the cadaver study was meant only to qualify the depth of cut, the amount of time between rounds was not deemed detrimental to the objective of the experiment.

Third Prototype (Translating System)

The amount of deflected reaming from the cortical femur trial resulted in a measured 1.03mm which is less than the projected 1.08mm given the size of the foam intramedullary canal. No measureable deflection was observed at the 20% length mark inside the IM canal. The prototype was able to achieve 3.75mm of deflected cutting during the cancellous foam model. Shaft contact was observed on the first rectangular cortical model indicating that adjustments to the flexibility to the reamer shaft may be necessary in future iterations and that the plunger had reached full engagement of the stainless steel plug. The full deflection of the reamer head was unable to be achieved in the second cortical trial due to the reamer shaft shearing during operation. This may likely be a result of the addition of a washer added between the weld and the plug to prevent binding. In the cortical model, an

imprint of the washer can be seen in **Figure 30** below. The results from each trial are tabulated in *Table 2* below.

Table 2: CUTTING DEPTHS OF THIRD PROTOTYPE

Foam Femur 20% Length	Foam Femur 30% Length	Cancellous Model	Cortical Model 1	Cortical Model 2
N/A	1.08mm	3.75mm	3.3mm	1.03mm

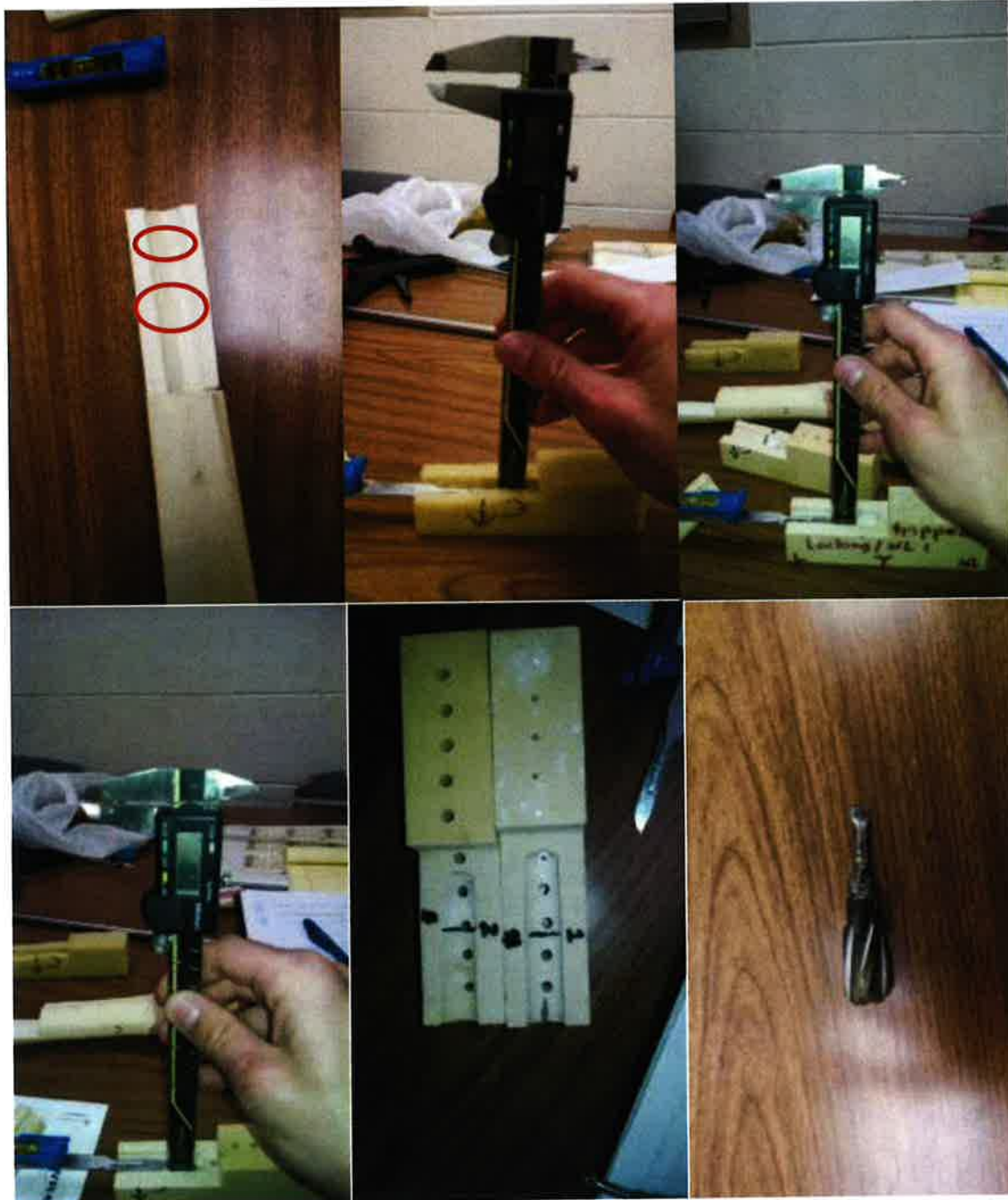


Figure 30: (Top Left) The 20% and 30% length cuts in the medial wall of the foam femur are shown. No measurable amount of deflected reaming was achieved at the 20% mark. A lateral cutting depth of 1.03mm was measured at the 30% mark which would theoretically equate to 2.9mm of lateral deflection before the adhesive between the reamer head and shaft failed. (Top Center) The cancellous foam model was cut to a depth of 3.75mm. The calipers read 4.4mm, but the thickness of the scalpel handle (.65mm) was subtracted to achieve the true displacement. (Top Right) In the first cortical foam model, the prototype reached a cutting depth of 1.78mm (accounting for the scalpel handle thickness) before the adhesive failed. (Bottom Left) The second cortical bone model only shows approximately 1mm of eccentric cutting. The reamer shaft failed in torsion possibly due to excessive force exerted by the plunger as it was advanced inside the plug. (Bottom Center) The first and second cortical bone models are shown with the locations of eccentric cutting marked in black. Note the wear on the proximal edge of the first model indicating the reamer head had reached full deflection. However, it is hypothesized that full deflection was not attained because the reamer head had become detached before full deflection could be reached. (Bottom Right) The distal section of the sheared reamer shaft is shown. The end was crimped in an attempt to remove the deformed

edge and reattach it to the remainder of the reamer shaft. Note the reamer head has been welded to the shaft. This may have caused a significant amount of torque to be placed on the shaft if the reamer head was attached to the shaft off center.



Figure 31: The third prototype exhibiting the separated reamer shaft is shown above. It is hypothesized that the washer used to prevent the weld from binding within the plug impinged on the inner wall of the canal. The shaft failed on the outer edge of the cortical model possibly indicating a bending moment was created between the edge of the stainless steel plug and the distal edge of the reamer head. The added distance from the weld and the shim would have increased the bending moment on the shaft as the plunger was driven into the plug. The plates held onto the attachment arms were included only to maintain alignment of the plunger and shaft within the attachment arms during operation.

V. Discussion

Two stages of displacement qualification were used in the development of the directional reamer system. First, the prototype was tested between two parallel plates, one of particle board and the other of clear acrylic to observe the displacement during reaming. As the project progressed, the parallel plate experiment evolved into the sawbones experiment. The second stage of testing involved a series of cadaver experiments conducted at the University of Louisville's Fresh Tissue Dissection Laboratory. A total of two cadaveric femurs were obtained to qualify the directional reaming system. The tests were analogous to those completed in the parallel plate and sawbones tests completed by Devicix, LLC.

Although the 14mm reamer deflection system design did allow for a measureable amount of lateral reaming, it failed to meet several design criteria. The bearing wear rate, addition of a new reaming technique, and the size restriction of the Stryker Bixcut reaming system all presented issues that prevented the current design from continuing towards manufacturing feasibility. This system was successful in achieving a proof of concept regarding medullary shaping and offered a solution to minimizing the amount of reamer chatter with the introduction of the follower sleeve.

The next iteration caused lateral reaming in a similar manner, but instead of using a conical surface to deflect the reamer head, a plunger was used to translate the reamer head away from the central axis. Through several design iterations, a manually controlled directional reaming system has been developed to laterally cut 3mm into the wall of the intramedullary canal. The system uses a plunger with a wedge shaped head which rides along a stainless steel plug to create a translating motion along the incline. A 4mm diameter stainless steel reamer shaft with a fixed 12mm reamer head rests on top of the plunger and is translated laterally as the plunger is advanced over the wedge of the plug. A stainless steel flexible channel connects the plug to a handle that remains external to the bone and encloses the plunger and the reamer shaft. The distal reamer shaft is seated in a "U" shaped plug containing a shallow incline through the middle. A plunger with a mating surface was advanced in a

manner similar to that of the follower sleeve. Since the plunger sits flush to the outer diameter of the plug, wall impingement of the shaft was not an issue as with the conical bearing designs. While this design was able to achieve the 3mm of lateral deflection in the foam models, a cadaver study was unable to be performed due to shearing of the reamer shaft. It is possible that the failure of the reamer shaft was due to several reasons. First, the addition of a washer to prevent the weld from binding within the plug added a significant amount of distance between the reamer head to the point at which the plunger first contacted the reamer shaft. This may have caused a bending moment which surpassed the reamer shafts point of failure. The reamer head was also not centrally aligned around the shaft due to manufacturing capabilities. This may have caused a stress concentrations along the reamer shaft increasing the bending moment during each rotation at the point the plunger first contacted the shaft. Despite the failure of the reamer shaft in this design, the translating reamer system proved to be a feasible design to pursue for future development after minor improvements are implemented.

VI. Conclusion

The translation prototype, while passing the initial foam model tests, still requires several improvements before clinical testing. It is suggested that the attachment arms (channel) be modified to be fully enclosed for at least part of the length or contain bridging segments between the user interface and the plug. This would increase the stability of the rotating shaft and lock the plunger into a track to prevent the risk of buckling as it is advanced within the plunger. The attachment arms must also be made flexible, likely using cuts along the upper and lower surface to allow it to flex with the shape of a bone similar to how the follower sleeve was designed in the other prototype. The plunger may also be made of steel instead of plastic (delrin) in order to prevent buckling when resistance is felt from laterally deflecting the reamer head. Another modification involves changing the shape of the reamer head from the standard cylindrical shape to one exhibiting a fishtail on the distal edge. This would create a more defined location for directional reaming to occur while stabilizing the cutting head as it contacts the canal wall. In order to accommodate the remaining project funds and timeline, only the components directly affecting the translation of the reamer shaft were machined and tested. Future experimentation is necessary to evaluate the optimal materials for the reamer shaft and plunger to minimize the effects of wear between the components. A more biocompatible combination may be necessary depending on the wear properties during operation. Through the development of the directional reaming system, a finalized design for meeting the clinical need has been generated. Though the final design requires minor improvement to enter clinical trials, the mechanics of the design meet the design objectives used to generate the design criteria. The translating system was able to ream 3mm laterally within a 12mm canal before shaft failure. After implementing the necessary design improvements, this model of deflecting reamer system will be advanced to human tissue testing.

Appendix A: Prototype Prints and CAD Drawings

12mm Conical Insert design

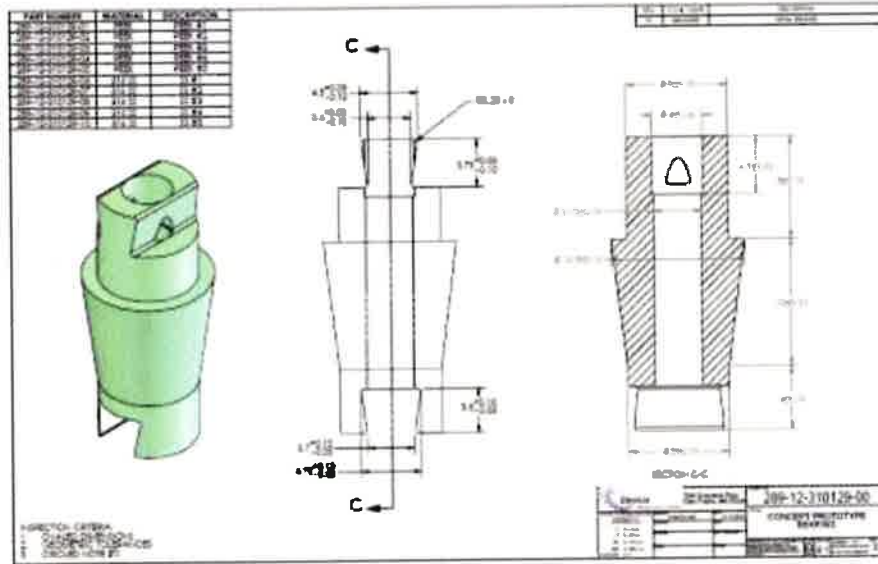


Figure 32: The conical insert was used in the first round of testing at Devicix. Both stainless steel and peek conical inserts were tested.

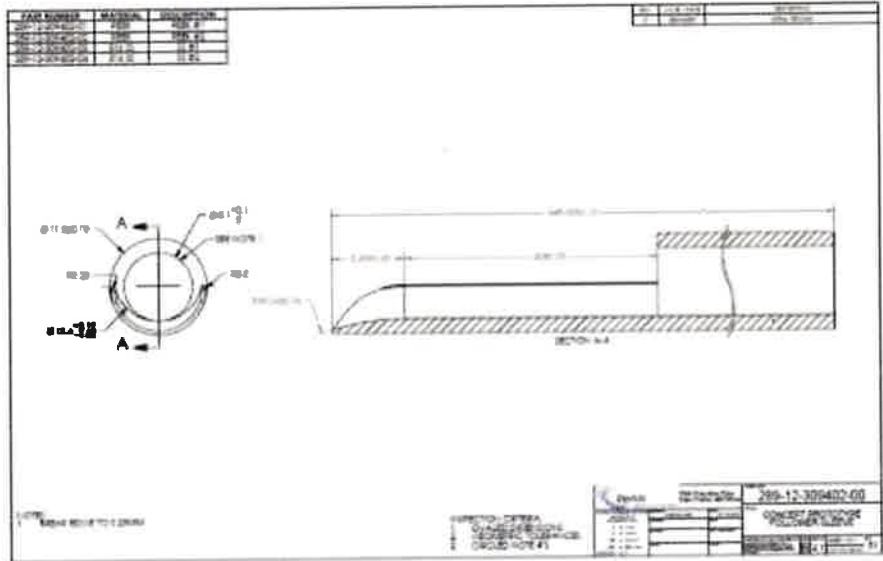


Figure 33: Dimensions for the first follower sleeve prototype are shown above.

14mm Conical Bearing Design

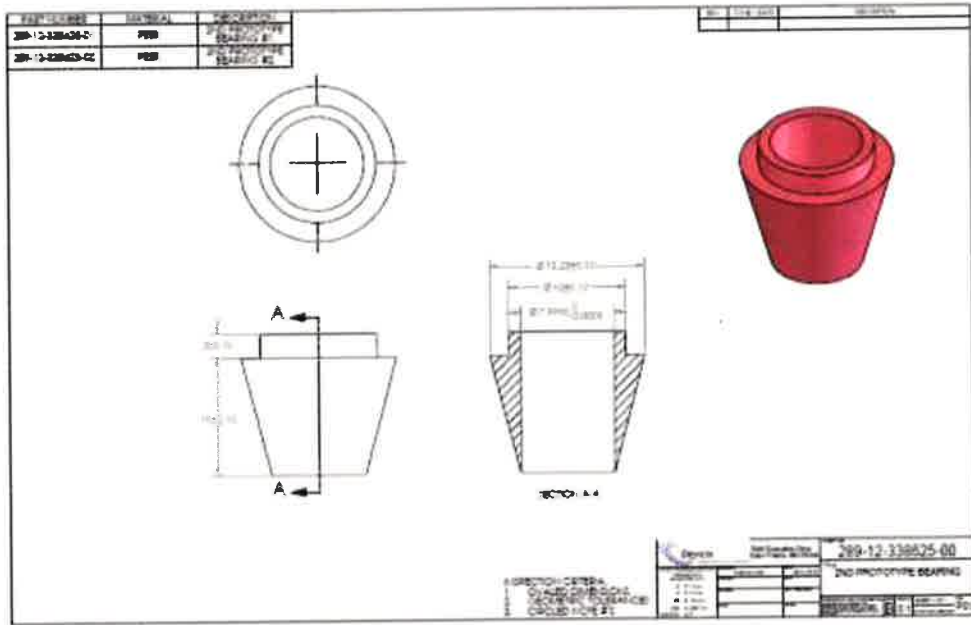


Figure 34: The 13.25mm conical bearing will be used in conjunction with a 14mm reamer head. This design allows for 3.25mm of lateral cutting.

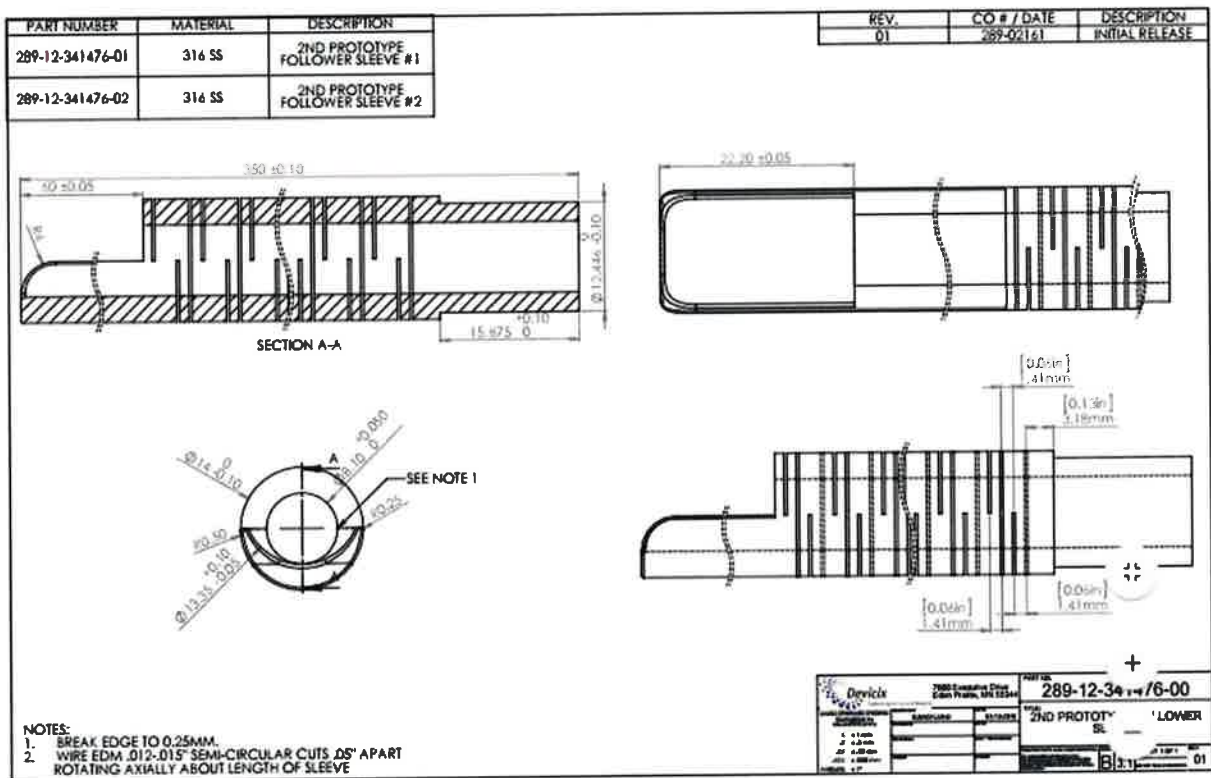
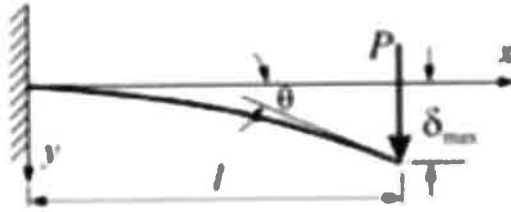


Figure 35: The flexible follower sleeve for the 14mm head displacement assembly is shown above. The length of the tongue has been increased to allow for greater flexibility along the reamer shaft.

Appendix B: Design Calculations

Displacement Calculations for 12mm conical insert:

Cantilever beam bending:



$$\theta = \frac{Pl^2}{2EI} \quad (\text{Eqn. 1})$$

$$\delta = \frac{Pl^3}{3EI} \quad (\text{Eqn. 2})$$

$$\theta = \frac{3\delta}{2l} \quad (\text{Eqn. 3})$$

Lateral displacement of reamer head:

Displacement of conical bearing: 1.25

Distal cutting head displacement: y

Length of follower sleeve: 30.0mm

Length from base of follower sleeve tongue to distal cutting head: 65.55mm



$$\sin \theta_{\text{Eqn.3}} = \frac{y}{65.55\text{mm}} \quad (\text{Eqn. 4})$$

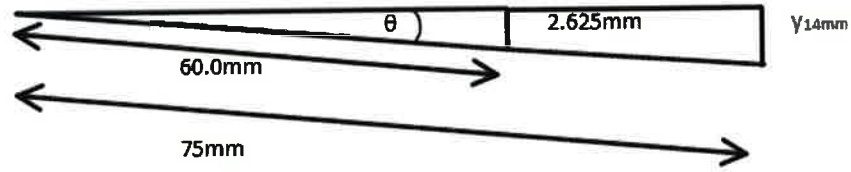
Displacement Calculations for 14mm Conical Bearing

Displacement of conical bearing: 2.625mm

Distal cutting head displacement: $y_{14\text{mm}}$

Length of follower sleeve tongue: 60.0mm

Length from base of follower sleeve tongue to distal cutting head: 75.0mm



$$\frac{2.625}{60} = \frac{y_{14mm}}{75} \quad (\text{Eqn. 5})$$

Follower Sleeve (14mm) Bending Stiffness

Bending Stiffness Calculations:

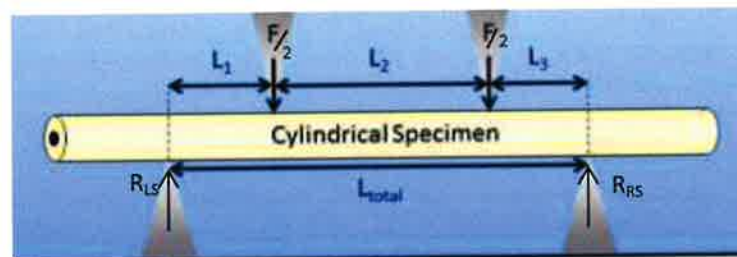
MTS displacement: 0-15mm

Displacement points chosen: 2mm, 12mm

Force at 2mm: $F = 4.611\text{N}$

Force at 12mm: $F = 16.102$

Calculation of Moment during four point bending of reamer shaft:



$$\Sigma F = -F + R_{LS} + R_{RS} \quad (\text{Eqn. 6})$$

$$\Sigma M_C = -\left(\frac{L_2}{2} \times \frac{F}{2}\right) + \left(\frac{L_{tot}}{2} \times R_{RS}\right) \quad (\text{Eqn. 7})$$

$$\delta = \frac{F}{2} \frac{(3L_{tot}^2 - 4L_1^2)}{24EI} \quad (\text{Eqn. 8})$$

Where

- $M_{C\ 2mm} = .2075\text{Nm}$
- $M_{C\ 12mm} = .7246\text{Nm}$
- $F_{2mm} = 4.611\text{N}$
- $F_{12mm} = 16.1026\text{N}$

Isolate and compare the values of EI in order find the number of flexibility slots necessary to develop a follower sleeve with a bending stiffness less than or equal to the stiffness of the reamer shaft.

Appendix C: Prototype Development Procedures

Torsional Experiment

Objective:

This experiment was conducted to observe the torsional stress created during directional reaming of a foam modeled long bone intramedullary canal. The torque values generated were then

compared to known torque limitations of the drilling systems used in standard operating rooms for reaming of lower extremity long bones. It is hypothesized that the torque values generated will not exceed the operational limits of the surgical driver systems currently used in the operating room.

Originally, a 12mm reamer was used to begin the experiment. However, the intramedullary canal of the foam femur had an inner diameter greater than 12mm. This caused the reamer head to “wobble” and resulted in erroneous torque readings. For this reason, the experiment was conducted using a 17.5mm reamer.

Materials:

- DE Walt power drill and battery
- 17.5mm flexible reamer system
- Stock polyethylene bar
- One cable four feet long
- Three 5lb weights
- A pulley on an adjustable stand
- Three C-clamps
- Bionix MTS machine and associated software
- Femoral foam bone model
- Standard fixed bench vice

Methods

Remove both epiphyses of the foam femur and clamp only a diaphysis of bone. Place the femur vertically into a vice on the base plate of the Bionix 858 MTS. In order to create deflection of the reamer head, drill a 10mm hole and a 4mm hole through a 63.5 X 38.1mm polycarbonate cube. Place the proximal end of the reamer shaft through the 10mm hole then secure it using the chuck into the power drill. Thread a cable through the 4mm hole then tie a set of weights at one end. Secure the other end of the cable to the plastic cube. The cable should rest over a pulley so that the weights hang vertically from the MTS base plate and cause a horizontal force to be applied to the reamer shaft; thus inducing a controlled amount of lateral deflection on the reamer head. Ream the IM canal of the foam femur

section using a 17.5mm reamer head while in the vice. Next, program the MTS machine to record time, torque, and shear force generated across the load cell. Use a 2500N load cell (or a smaller load cell to capture better resolution if available) with the resolution set to 30N to most accurately record the program data presented in **Figure 34**. Place the reaming assembly over the foam IM canal, and activate the power drill to full power. Lower the reaming assembly until the reamer head is 2cm below the top edge of the foam femur. Zero the MTS machine. Attach a 44.5N weight to induce deflected reaming, but do not allow the weight to put tension on the cable until the MTS program is activated. Once the MTS machine begins recording data, gradually allow the 44.N weight to hang from the cable to cause the reamer shaft to bend. Maintain power drill activation for a minimum of 10 seconds. Once deflected reaming has occurred, remove the tension from the cable to allow the reamer shaft to straighten, and retract the reaming assembly from the IM canal. Import the data following the experiment into Microsoft Excel. Repeat the experiment for a total of three trials with 44.5N and three trials with 66.7N to observe the torque and lateral force values possible during deflected reaming.

Results

A substantial amount of noise remained through the trials. This may possibly be due to use of the load cell near its lower operational limits. Reamer shaft “wobble” was reduced to a negligible amount due to implementation of the 17.5mm reaming system. Data is depicted graphically below, and although it shows a substantial amount of noise, several conclusions may be drawn. From the data collected, it may be inferred that while the data is noisy, it was consistently less than the operational torque limits specified in standard surgical drilling and reaming systems which range ordinarily from 5.5-20Nm of torque[1,2]. It can also be seen from the data presented that the increase in weight displacing the reamer shaft causes higher torque values while reaming directionally. Maximum torque values captured during trials 1, 2, and 3 falls primarily between 1.5-2Nm while the values from 4, 5, and 6 are found in the 2-3Nm range. It is hypothesized that the torque values of the opposite sign are a result of

the sample reverberating in the opposite direction during reaming due to the inability to completely stabilize the MTS load cell, which creates the noisy plots as shown in **Figure 34**. During trial two, the drill was moved out of alignment slightly during removal of the reaming assembly. This resulted in erroneous torque values between the 35 and 40 second interval.

Conclusion

Directional reaming of intramedullary long bones will not induce torsional loads which surpass the operating limits of standard surgical reaming systems. This experiment may yield more accurate results if repeated with a working prototype of a directional reaming assembly utilizing a follower sleeve and displacement apparatus. However, it is anticipated that the prototype will have lower torque values than standard reaming since less frictional force resulting from less contact area between the reamer head and the intramedullary canal will be present as the reamer head is deflected.

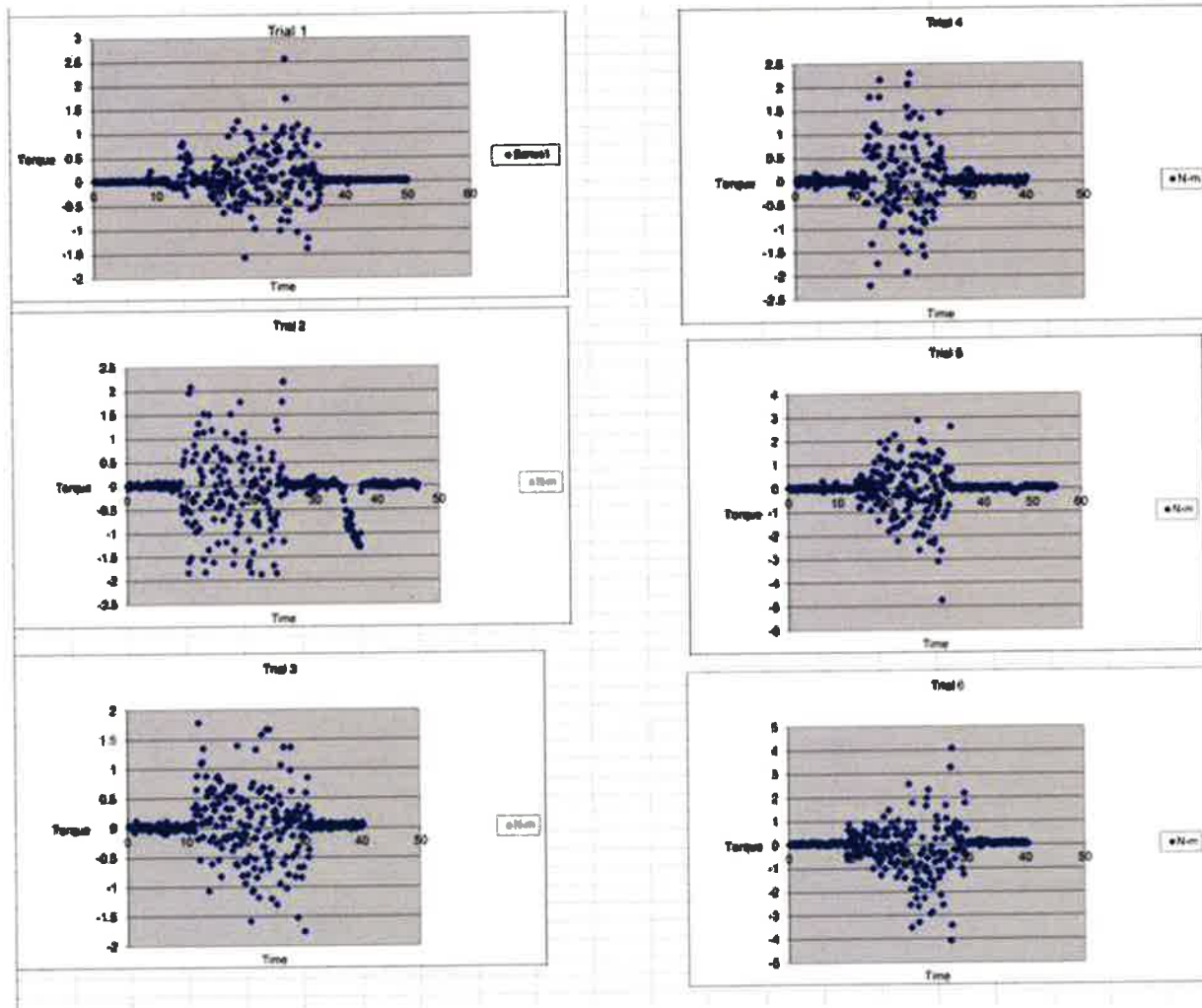


Figure 36: REAMER TORQUE VALUES. Trials 1,2, and 3 were conducted using 10lbs. Trials 4,5, and 6 were conducted using 15lbs. The maximum torque values for each trial did not exceed reamer torsional limits (4.63Nm). Data taken during the trials occurs ten seconds into the trial. This delay is due to the time taken to insert the drill into the intramedullary canal.

Follower Sleeve Finite Element Analysis

The development of the flexible follower sleeve was completed using SolidWorks 2015x64 Academic Edition. The objective of the finite element analysis study was to optimize the number of cuts within the follower sleeve to achieve sufficient flexibility while sustaining the axial compression generated during reamer deflection. Since the original part file was created in SolidWorks, the file was imported without any changes to the file. Before running the analysis, the target stiffness was achieved by calculating the bending stiffness (EI) from the flexible Stryker Bixcut reaming shaft (See Appendix B-

Follower Sleeve Bending Stiffness). The shaft was placed under four point bending as shown in **Figure 35** and a Bionix 858 MTS test system was used to place a vertical load on the shaft. The MTS machine was programmed to collect force data as a result of input displacement data from 0-15mm of vertical displacement. From this data, the forces correlating to two different amounts of displacement were isolated. Two points of displacement were used to compare the stiffness behavior and choose a worst case for finding a target stiffness for the FEA simulation in SolidWorks. The two points chosen were 2.0mm of displacement and 12.0mm of displacement. At these two points of displacement the forces were shown to be 4.611N and 16.10N respectively.



Figure 37: Shown above is the experimental setup for generating a four point bending load on the Stryker flexible reaming shaft. This method of loading allowed the team to isolate the bending stiffness of the flexible shaft (Eqn. 6-8). In order to develop the flexible follower sleeve, this experiment was replicated in SolidWorks 2015 Academic Edition.

After importing the part file of the follower sleeve created by Devicix and the university team, a new nonlinear study was created. The material was chosen to be AISI 316 Stainless Steel to match the

material to be used in the finished prototype. Under the *Connections* option, the *No Penetration* contacts set was chosen to ensure that the part file did not yield erroneous results due to self-contact during simulated deformation. Next, the fixture locations and types were selected. In order to create an accurate fixture replicating the lower two points of the four point bending setup, two 100.0 μ m diameter cylindrical faces were cut into the cylindrical surface of the follower sleeve (see **Figure 36**). The fixtures were placed on these two cuts as cylindrical face fixtures with translation limits of 0.00mm radially, axially, and laterally. The area of each cut made is 1.07mm² with a negligible total volume. The cuts are equidistant from the centroid of the sleeve and 233.41mm apart from each other. This distance was chosen to prevent the fixture cuts from interfering with the flexibility cuts along the length of the sleeve.

After the fixture locations had been set, the appropriate load was calculated (Eqn. 6 and 7) using the moment generated during the four point bending of the Stryker shaft. Next, the forces were set within the FEA on the surfaces normal to the top plane of the follower sleeve. From the four point bending exercise completed using the MTS machine, the forces to be applied to the follower sleeve were translated into the FEA as 17.29N for the 12mm displacement and 8.452N for the 2mm displacement. The pair forces were set equidistant from the centroid of the sleeve at 82.36mm apart. A solid, curvature based mesh was then generated with a maximum element size of 2mm and a minimum size of 1mm. The mesh details can be found in Appendix D. The simulation was run and the results were captured in the report found (Appendix D). Since the higher stiffness ratio (EI) was higher when displacing the shaft 12mm, this ratio was used as a worst case scenario for comparing the flexible shaft to the follower sleeve design.

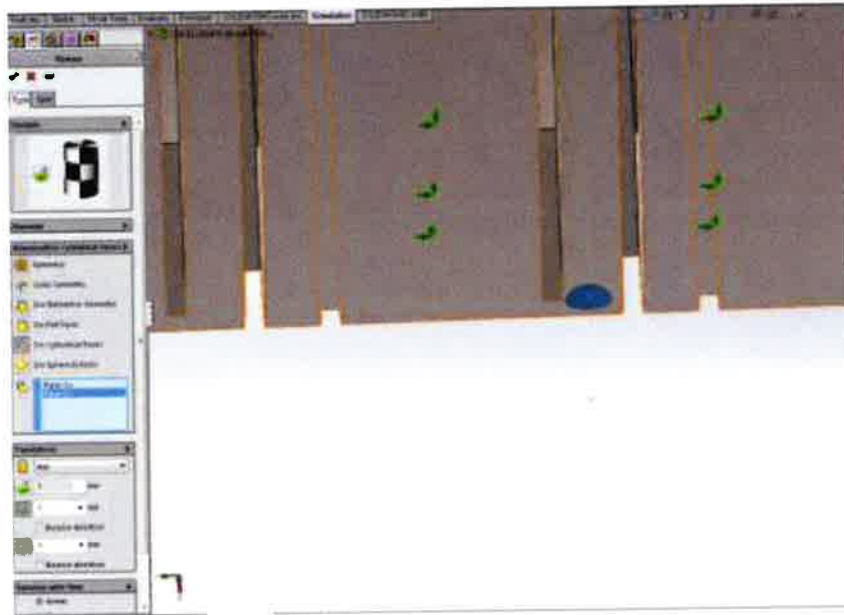


Figure 38: One of two fixture cuts is shown as the highlighted cylindrical region in the close-up of the follower sleeve in SolidWorks.

After the force magnitudes were chosen, the simulation was run iteratively until the bending stiffness of the proposed follower sleeve was just below the bending stiffness of the flexible Stryker shaft. The bending stiffness of the follower sleeve was manipulated by changing the number of cuts along the sleeve in each quadrant. As the number of cuts was reduced, the stiffness ratio decreased. Three complete iterations were achieved. From the simulations, it was concluded that the number of cuts could be reduced by five in each quadrant for a total of 20 fewer cuts (48 in each quadrant, 49 in the quadrant perpendicular to the tongue). The resulting EI ratio between the flexible shaft and the proposed follower sleeve design was 0.501:0.653. This result is significant since wire EDM was used to create the cuts along the follower sleeve and minimizing the number of cuts reduced manufacturing time and costs.

Appendix D: Follower Sleeve Finite Element Analysis Report



Figure 39: Simulated image of the second prototype's follower sleeve is shown above.

Simulation of 289-12 341476-00 with FEA

Date: Friday, June 17, 2016

Designer: Solidworks

Study name: Nonlinear 1

Analysis type: Nonlinear - Static

Description


Optimization of follower sleeve flexibility cuts

Model Information



Model name: 289-12-341476-00 with FEA
Current Configuration: Sleeve 1

Solid Bodies

Document Name and Reference	Treated As	Volumetric Properties	Document Path/Date Modified
Cut-Extrude15 	Solid Body	Mass:0.229603 kg Volume:2.87004e-005 m ³ Density:8000 kg/m ³ Weight:2.25011 N	C:\Users\aaхоep01\Desktop\joe's fea\289-12-341476-00 with FEA.SLDPRJ Jun 17 13:11:36 2016


Study Properties

Study name	Nonlinear 1
Analysis type	Nonlinear - Static
Mesh type	Solid Mesh
Start time	0 Seconds
End time	1 Seconds
Time increment	Auto stepping
Large displacement formulation:	On
Update load direction with deflection:	Off
Large strain formulation:	Off
Save data for restarting the analysis	Off
Thermal Effect:	On
Thermal option	Include temperature loads
Zero strain temperature	298 Kelvin
Solver type	FFEPlus
Incompatible bonding options	Simplified
Control technique:	Force
Iterative technique:	NR(Newton-Raphson)
Integration Method	Newmark
Result folder	SOLIDWORKS document (C:\Users\aaheop01\Desktop\joe's fea)

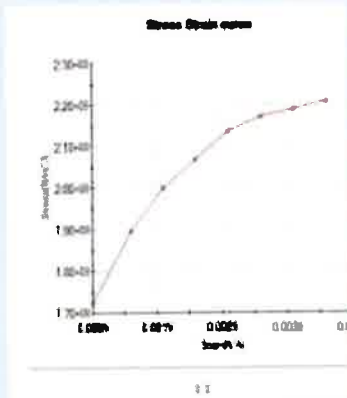
Units

Unit system:	SI (MKS)
Length/Displacement	mm
Temperature	Kelvin
Angular velocity	Rad/sec
Pressure/Stress	N/m ²

Material Properties


Model Reference	Properties	Components
	<p>Name: AISI 316 Stainless Steel Sheet (SS)</p> <p>Model type: Plasticity - von Mises</p> <p>Default failure criterion: Max von Mises Stress</p> <p>Yield strength: 1.72369e+008 N/m²</p> <p>Hardening factor (0.0-1.0; 0.0=isotropic; 1.0=kinematic): 0.85</p> <p>Elastic modulus: 1.93e+011 N/m²</p> <p>Poisson's ratio: 0.27</p> <p>Mass density: 8000 kg/m³</p> <p>Thermal expansion coefficient: 1.6e-005 /Kelvin</p>	<p>SolidBody 1(Cut-Extrude15)(289-12-341476-00 with FEA)</p>


Curve Data:



Stress Strain curve

Loads and Fixtures

On Cylindrical Faces-1		<p> Entities: 2 face(s) Type: On Cylindrical Faces Translation: ---, 0 rad., 0 Units: mm </p>		
Resultant Forces				
Components	X	Y	Z	Resultant
Reaction force(N)	-0.691758	0	-7.45058e-008	0.691758
Reaction Moment(N.m)	0	0	0	0

Load name	Load Image	Load Details
Force-1		<p> Entities: 4 face(s) Type: Apply normal force Value: 17.294 N </p>

Mesh information

Mesh type	Solid Mesh
Mesher Used:	Curvature based mesh
Jacobian points	4 Points
Maximum element size	2 mm
Minimum element size	1 mm
Mesh Quality	High

Mesh information - Details

Total Nodes	102647
Total Elements	53388
Maximum Aspect Ratio	221
% of elements with Aspect Ratio < 3	87.3
% of elements with Aspect Ratio > 10	0.702
% of distorted elements(Jacobian)	0
Time to complete mesh(hh:mm:ss):	00:00:11
Computer name:	ORTHO-VOORLAB



Resultant Forces

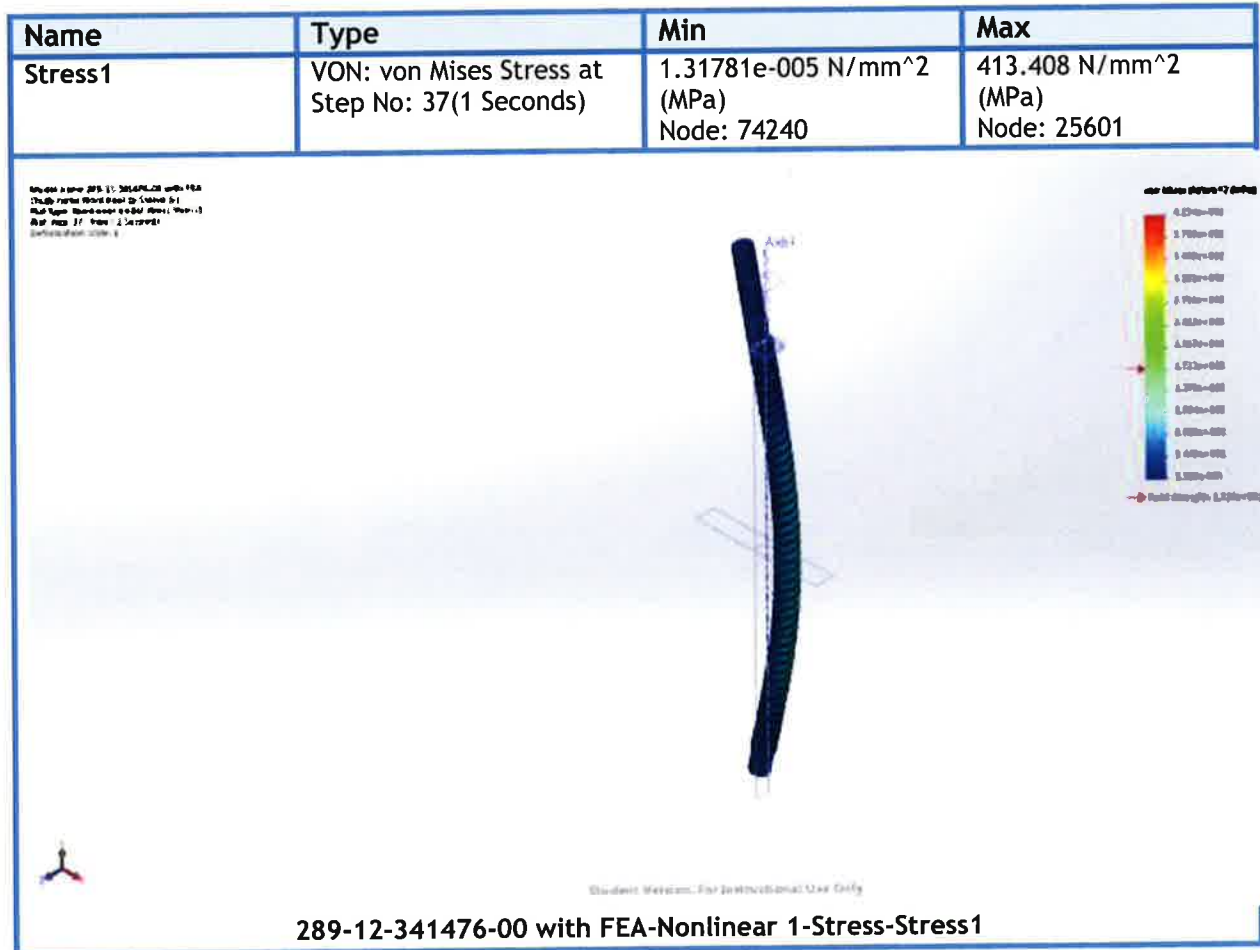
Reaction forces

Selection set	Units	Sum X	Sum Y	Sum Z	Resultant
Entire Model	N	-0.691758	0	-7.45058e-008	0.691758

Reaction Moments

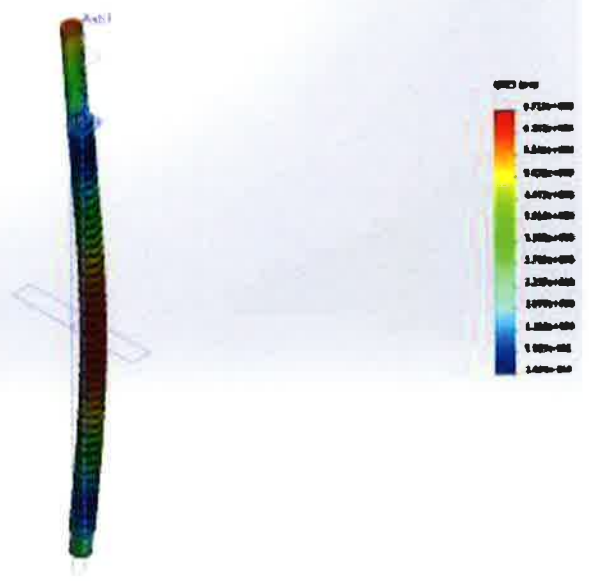
Selection set	Units	Sum X	Sum Y	Sum Z	Resultant
Entire Model	N.m	0	0	0	0

Study Results



Name	Type	Min	Max
Displacement1	URES: Resultant Displacement at Step No: 13(0.621875 Seconds)	0.000160441 mm Node: 7105	6.70987 mm Node: 36950

Model name: 289-12-341476-00 with FEA
 Study Name: Displacement1 (0.621875 s)
 Run Time: 15.996 s (0.621875 seconds)
 Surface Element: 2048



Student Version. For Instructional Use Only.

289-12-341476-00 with FEA-Nonlinear 1-Displacement-Displacement1

Name	Type	Min	Max
Strain1	ESTRN: Equivalent Strain at Step No: 13(0.621875 Seconds)	4.42028e-010 Element: 7555	0.0275812 Element: 14528

Model name: 289-12-341476-00 with FEA
 Study Name: Strain1 (0.621875 s)
 Run Time: 15.996 s (0.621875 seconds)
 Surface Element: 2048



Student Version. For Instructional Use Only.

289-12-341476-00 with FEA-Nonlinear 1-Strain-Strain1

Name	Type	Min	Max
Copy[1] Stress1	VON: von Mises Stress at Step No: 13(0.621875 Seconds)	0.000152122 N/mm ² (MPa) Node: 82034	284.547 N/mm ² (MPa) Node: 25011

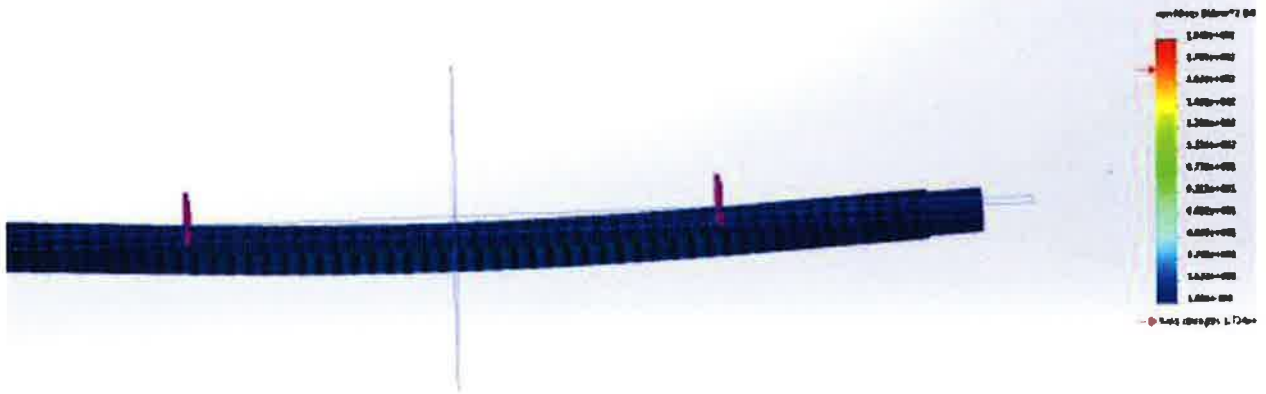
Model name: 289_12_341476-00 with FEA
 Study Name: Nonlinear 1-Strain-Strain1
 Step Name: Nonlinear 1-Strain-Strain1 (Copy 1) Step 13
 Step Type: Nonlinear 1-Strain-Strain1
 Substep Name: 13
 von Mises (Effective) Stress (MPa) = 12.28 N/mm²



Student Version. For Instructional Use Only

289-12-341476-00 with FEA-Nonlinear 1-Stress-Copy[1] Stress1

Model name: 2015-11-261501-02 with P&S
Shell type: Shell mesh 15 - Shell 2-1
Mesh type: Hexahedral element shape: Tetra-10
Ref. msg: 15 Nov 2 10:00 AM
SurfaceMesh: 2768 1



Student Version, For Instructional Use Only

Image-1

Conclusion

A total of 49 cuts in the quadrant aligned with the follower sleeve tongue and 48 cuts in the remaining three quadrants are recommended as a result of this study. Note the finite element analysis software package available in SolidWorks 2015-2016 Academic Edition is an estimation and subject to error within the mesh.

Appendix E: Cadaver Trial 1 Fluoroscopic X-rays

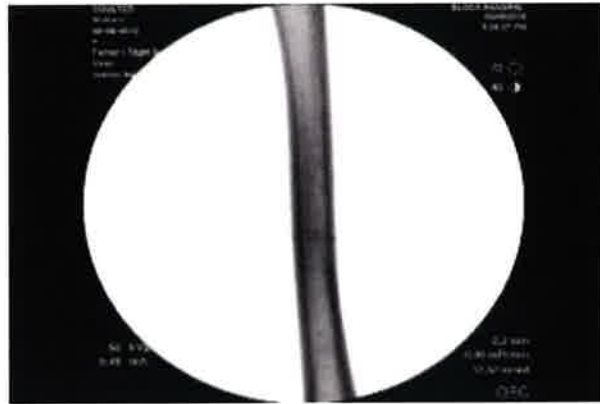


Figure 40: Lateral view of the deflected cut is located just above the wire ring used to mark the directionally reamed location.

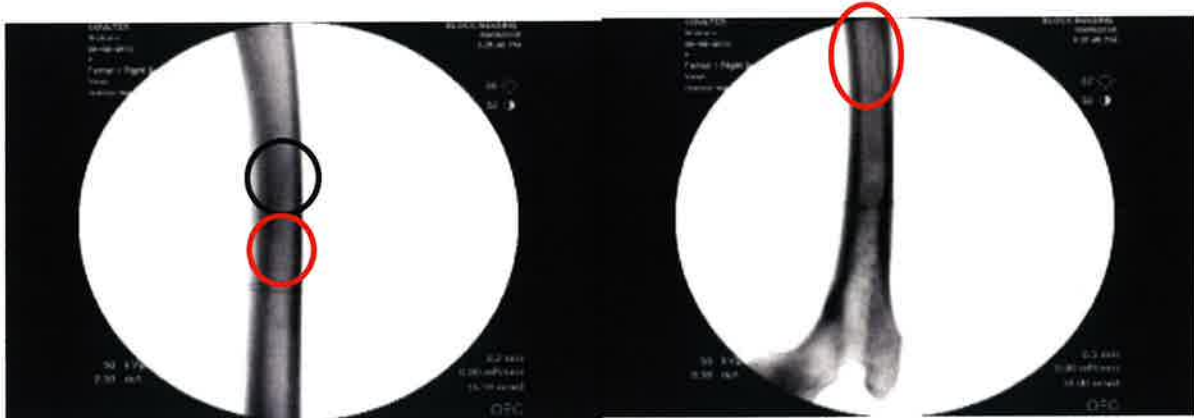


Figure 41: (Left) An anterior-posterior view of the femur is shown with the 50% length cut circled in black and the 40% length cut circled in red. (Right) A lateral shot of the deflected cut is shown above. The directionally reamed location is circled in red. The 25% length cut is outlined in this image by the wire.

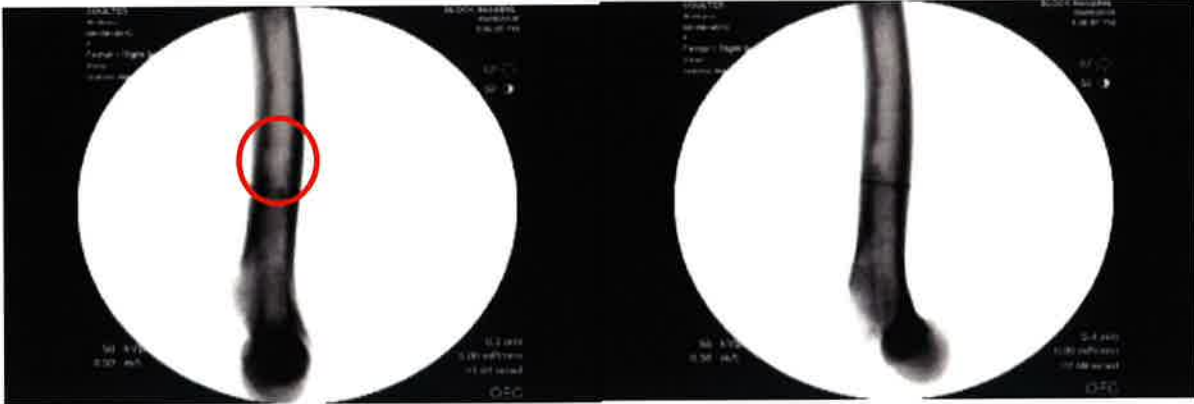


Figure 42: (Left) The anterior-posterior view of the directionally reamed location can be seen circled in red just above the wire marker. (Right) The lateral view of the same cut is shown just above the wire marker.

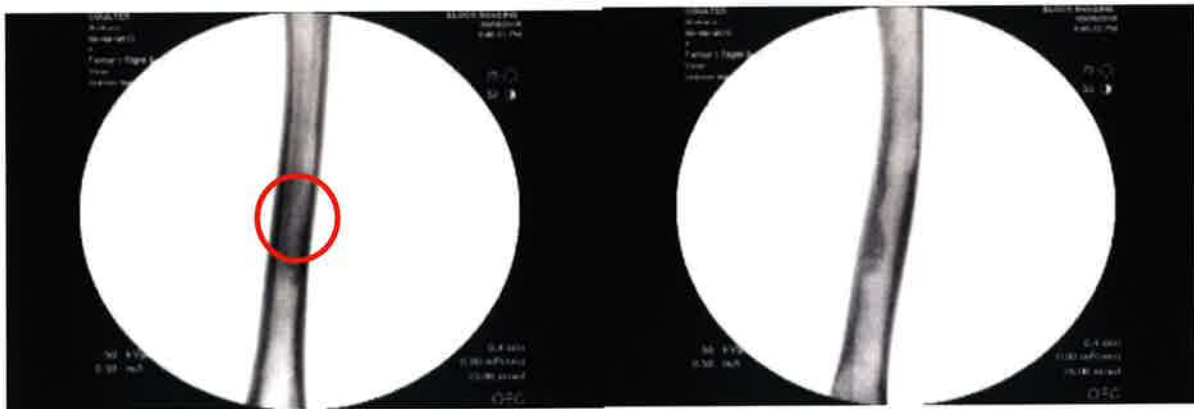


Figure 43: (Left) In the anterior-posterior view the reaming assembly was returned to the 50% location to attempt a circumferential cut. (Right) The same cut is shown in the lateral view. Note the reamed material still inside the canal.

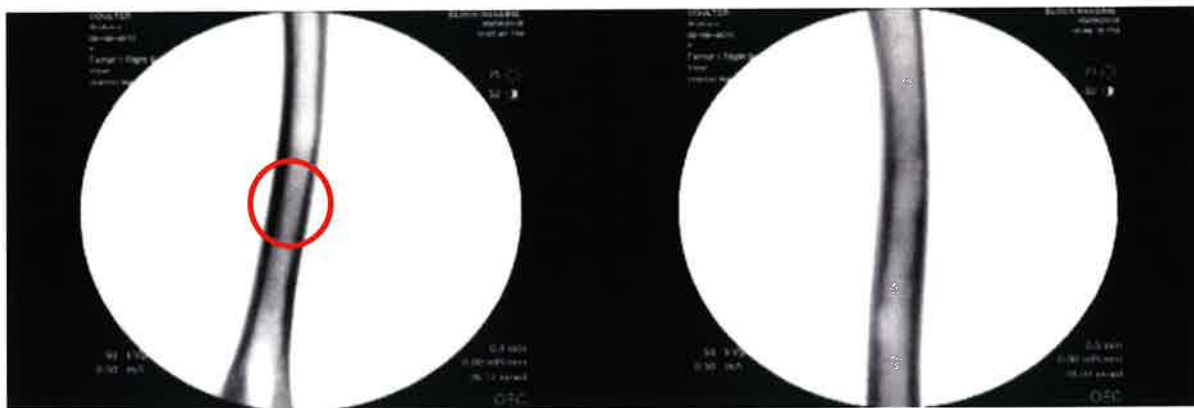


Figure 44: (Left) Anterior-Posterior image shows the same 50% location of the attempted circumferential cut after the 14mm reamer head had been passed through without deflection in order to clear the reamed debris. (Right) The same location is shown in a lateral view

Appendix F: Miscellaneous Information

Nonexclusive License for Electronic Thesis and Dissertations

University Libraries at University of Louisville ("UL") and Author wish to enter into a licensing arrangement in order to preserve the thesis or dissertation Work of Author ("the Work") identified and described more fully herein,

Directional Reaming of the Intramedullary Canal: An Innovation in Intramedullary Shaping

and to make the Work accessible and widely available for dissemination through and using a range of extant and later developed technologies and formats consistent with the goals of scholarship and library practices in the scholarly community.

To that end:

1. Author grants to UL, its agents, assigns, and necessary contractors or third parties, nonexclusive, irrevocable, and worldwide rights and license to reproduce, distribute, prepare collectives, compilation, and derivatives, perform, display, and otherwise alter and modify the Work consistent with this license and the needs and requirements of relevant technologies used to effect the intent of this license as determined by UL at its sole discretion. Author also waives any "moral rights" that may exist in elements of the Work. Author otherwise retains all other rights in the Work and bears sole responsibility for complying with copyright and other legal requirements in the U.S. and elsewhere as they may govern the ownership and enforcement rights of Author.
2. Author makes the following representations and warranties regarding the Work:
 - a. The Work is the sole and original work of Author.
 - b. Author has full authority, capacity, and power to enter into this license.
 - c. The Work contains no audio, information, programming, textual material, video, or other content or component that (1) is defamatory, (2) breaches or otherwise violates any existing agreements between Author and another party including confidentiality agreements and like arrangements, (3) infringes any intellectual property rights, including copyright, patent, trademark, trade secret or other rights of a third party, (4) and that any inclusion of copyrighted material into the Work was made with written permission or is consistent with a "reasonable and good faith" application of fair use as applied and codified in 17 U.S.C. §107 of United States law.
3. Author agrees to hold UL harmless and to indemnify UL for reasonable attorney fees, costs, and damages in the event of a claim or allegation arising from violations of clause 2 or arising from the breach of any representations and warranties expressed in this license.
4. Author acknowledges that UL may remove or otherwise disable the Work under the force of law, for allegations of infringement or other unlawful occurrences, or due to circumstances beyond UL control and that UL makes no representations or warranties whatsoever about the ETD program or whether the Work will be included in it or any iterations and versions of it today or in the future.

Author Signature: 

Printed Name: Richard Joseph Ackermann III

Date: 04May2017

APPOINTMENT OF MEMBERS OF THE EXAMINATION COMMITTEE
UNIVERSITY OF LOUISVILLE
J. B. SPEED SCHOOL OF ENGINEERING

5/4/2017

MEMO TO: Academic Affairs Office J. B. Speed School of Engineering
FROM: Dr. Michael Voor, Associate Professor in Orthopedic Surgery
SUBJECT: Appointment of Members of the Master of Engineering Examination Committee for
Richard Joseph Ackermann III
THROUGH: Dr. Ayman El-Baz

I. CONSTITUENCY OF EXAMINATION COMMITTEE

It is recommended that the following individuals be officially designated as members of the Master of Engineering Examination Committee of subject M.Eng. candidate. Each of these persons has been contacted, and has agreed to serve on the Examination Committee (see page 1 for more detail on constituency of the committee):

(Name, Department)

1. Dr. Michael Voor Thesis Director
2. Dr. Glen Prater Member
3. Dr. Thomas Roussel Member

In addition to the foregoing membership of the Examination Committee, it is requested that the following committee representatives from outside Speed School, each of whom has agreed to serve, be appointed as Members of the Examination Committee:

1. Dr. David Seligson External Member

(Name)

550 S Jackson St, Louisville, KY 40202

(Mailing Address of External Member)

II. M.ENG. PROJECT DESCRIPTION

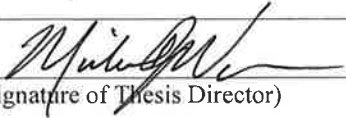
A brief description of the proposed M.Eng. Project is as follows:

The newly developed reaming system is intended to allow the surgeon to be more selective in where the reamer head cuts while shaping the inner wall of the intramedullary canal to avoid or target certain areas of the canal. Development of the directional reaming system included two prototypes with three sets of experiments to quantify the success of the designs. The first experiment resulted in a prototype unable to achieve the specified 3mm of lateral cutting depth.

APPENDIX II
(continued)

A tentative title (10 words or less) of the proposed M.Eng. Thesis is:

Development of a Directional Bone Reaming System



(Signature of Thesis Director)

III. APPROVAL BY DEPARTMENT CHAIR

The Thesis Director has conferred with me relative to the investigation, thesis topic and committee membership of the indicated student, and I concur with the recommendations.



(Signature of Department Chair)

General Instructions:

The student in collaboration with the Thesis Director should prepare this form: original to the Department Chair, copy retained by the student, and one copy for the Thesis Director's file.

Full-time students must submit the project description and constituency of the Master of Engineering examination committee according to the specific dates in Appendix I.

Part-time students must submit the project description and constituency of a Master of Engineering examination committee not later than one calendar year prior to the student's expected date of graduation.

Approval form to be distributed by Department Chair to M.Eng. candidate, thesis director, committee members, and Academic Affairs Office.

ORAL EXAMINATION REQUEST
UNIVERSITY OF LOUISVILLE
J. B. SPEED SCHOOL OF ENGINEERING

5/4/2017

MEMO TO: Academic Affairs Office

FROM: Dr. Michael Voor

SUBJECT: M.Eng. Oral Examination and Thesis Defense for Richard Joseph Ackermann III

1. The oral examination and thesis defense of subject degree candidate will be held on Friday, April 28th, 2017, at 10:00a.m.in the Orthopaedic Conference Room of the Ambulatory Care Building.

2. The title of the M.Eng. Thesis is:

Directional Reaming of the Intramedullary Canal: An Innovation in Intramedullary Shaping



(Signature of Thesis Director)

THE STUDENT IS RESPONSIBLE FOR DISTRIBUTION OF THESE COPIES

Copies to: 1) Department Chair Dr. Ayman El-Baz

2) Thesis Director Dr. Michael Voor

3) Committee Member Dr. Thomas Roussel

4) Committee Member Dr. Glen Prater

5) Committee Member Dr. David Seligson

ORAL EXAMINATION RESULTS
UNIVERSITY OF LOUISVILLE
J. B. SPEED SCHOOL OF ENGINEERING

5/4/2017

MEMORANDUM TO: Academic Affairs Office

FROM: Dr. Michael Voor

SUBJECT: M.Eng. Oral Examination and Thesis Defense For Richard Joseph Ackermann III

1. The oral examination and thesis defense of the above named degree candidate was held on Friday, April 28th of 2017 in the Orthopaedic Conference Room in the Ambulatory Care Building.
2. The examination and defense began at 10:00a.m. and was concluded at 11:30a.m.
3. The candidate **PASSED** the oral examination and thesis defense.
4. Qualifications or clarifying statements considered to be important by the Thesis Director (Optional):



(Signature of Thesis Director)

Copy to: Department Chair

List of Figures

Figure 1[5]: A healed tibia two years after fracture operation is shown above with a prospective need for directional reaming system to more accurately follow the intramedullary canal.....	11
Figure 2: Shown above is an anterior view of a tibial fracture with a reamer system and guidewire enabling fracture reduction. Use of a directional system in this case would allow for a more accurate navigation of the fracture site increasing the success rate of the operation.	12
Figure 3: A clamshell osteotomy is illustrated above. A segment of the shaft is extracted, cut, and replaced to form a more normal anatomical position.	13
Figure 4 [13]: The dissected tibiotalar joint is shown above with the guidewire hole circled in black. Notice the location of the hole relative to the center of the talus. This image indicates the impending structural damage that may be caused to the talus and subsequently calcaneus once the reaming procedure for nail insertion begins.	16
Figure 5: A lateral fluoroscopic radiograph from the study by Lowe et al. is shown depicting the location of a 12mm reamer at the tibiotalocalcaneal joint. By deflecting the reamer head posteriorly in this circumstance, less bending stress may be placed on the components of the talocalcaneal region as well as a better alignment may be achieved in order to more accurately enter the tibial IM canal ensuring optimal nail placement.	17
Figure 6[23]: Progression of osteomyelitis is illustrated in the figure above. Note the devascularization shown in the first stage which along with a biofilm formation greatly reduces effectiveness of antibiotic treatment. For this reason, surgical debridement is often necessary.	19
Figure 7: Lateral Tibia of a 46-year old female showing a pocket of sequestra as a result of repeated infection highlighted by the black arrow. Pockets such as the one shown pose a problem for standard reaming operations concerning the structural integrity of the cortical wall as the reamer head passes the infected site.[3].....	20
Figure 8: The conical insert design (green) is shown above. In this design, both peek and stainless steel inserts were manufactured as well as follower sleeves (yellow) in both materials.	25
Figure 9: the two follower sleeves and conical inserts are shown above. Experimentation has shown that deflected reaming has no damaging effects on either the peek or the stainless steel parts.	26
Figure 10: The distal end of the stainless steel follower sleeve with the slots cut for flexibility is shown above. It is important to note the relief cut into the distal portion of the tongue. This relief gives a smooth transition of the sleeve over the conical bearing when reaming laterally. The remainder of the tongue matches the outer diameter of the reamer shaft in order to add stability, provide a more economic manufacturing geometry, and minimize the chances of the reamer head walking or shaking during operation.....	28

Figure 11: Shown above is the conical bearing and flexible follower sleeve design for the second round of testing. The flexibility slots can be seen in the right hand side of the assembly (shown in purple).....	29
Figure 12: An exploded view of the distal portion of the directional reaming system is shown. Note the Aluminum grit blasted region (2) on the reamer cutting head (1) as well as the peek conical bearing with the added stainless steel shim (3) to separate the bearing from the cutting flutes of the reamer head. The flexible follower sleeve (4) is shown above the reamer shaft (5) which contains a spiral cut to induce flexibility (not shown).	29
Figure 13: The test setup for the three trials is shown above. The image on the right shows the position of the reamer system between the plates with the follower sleeve clamped to the MDF board. In this figure, trial two containing the peek follower sleeve and stainless steel conical insert is shown in the fixture.	37
Figure 14: The completed prototype is shown above. Note: this system is cannulated for inclusion of a guidewire (not present).....	39
Figure 15: Devicix saw bone test is pictured above.....	41
Figure 16: (Left) The second sawbones trial is shown above. The epiphyses were removed for this round of testing to allow the operator to more easily gage the distance of the reamer head down the IM canal of the sawbone. (Middle) A close-up view of the deflected cut is shown in the coronal plane. The sawbone experienced minor cracking during the cutting along the coronal plane to expose the deflected cut. This had no effect on the measured results of the experiment. (Right) The depth of maximum deflection was 5.74mm. No walking or otherwise detrimental effects of deflecting the reamer head are evident from the results meaning a successful experiment. From these results, the directional reaming system was proposed to be tested in a cadaver study.....	42
Figure 17: All parts were again visually inspected for wear and structural damage. Scuff marks and discoloration can be seen on the inner diameters of the peek and stainless steel follower sleeve tongues. Although not clearly visible from the available pictures, slight discoloration was also present on the peek conical bearing displayed on the right.	55
Figure 18: Circled above is the location of deflection reaming using the 14mm reamer head. Only a depth of 2.3mm was achieved from this trial.....	56
Figure 19: (Left) The first sawbones trial is shown above. The deflected cut did not reach the cortical shaft of the sawbone; however, a maximum depth of 3.55mm was achieved. (Middle) A representation of the reamer's deflected position is given within the site of the deflected cut. (Right) The method of measurement is shown above.	57
Figure 20: The modified reamer head on the left is unused and shows the amount of wear the reamer used in the sawbones experiment (right) sustained.	57
Figure 21: (Left) The maximum deflection achieved from the first round of cadaver testing was 1.66mm. (Right) The deflected cut is circled above. Upon removal of the anterior section of cortical bone, it was found that the anterior and posterior walls of the IM canal were irregularly shaped and did not present a smooth surface for easily observing a clean deflected cut into the	

IM canal wall. For this reason, the team performed the second round of testing on the medial and lateral walls of the canal.	59
Figure 22: (Left) The second round of deflected reaming took place in the circled area shown above. The cut was made in the distal region of the femoral diaphysis on the medial wall. The deflected cut was exposed using an oscillating bone saw to create a quarter length cut along the diaphysis. (Right) A close up image of the deflected cut is shown in the darker shaded side of the image. The deflected cut is called out in red.....	59
Figure 23: The maximum amount of deflection was found to be 1.04mm. Thus, this model of a directional reaming device did not achieve the qualifying criterion of 3mm of lateral deflection as dictated in the experiment objectives. The main contributing factor to this result is bearing wear due to the friction between the stainless steel follower sleeve and the peek bearing. A possible solution to this issue is reversing the materials of the follower sleeve and bearing. However, a more practical solution may be found with the next iteration of the directional reaming system involving a canal plug and reamer shaft saddle.	60
Figure 24: The peek bearing sustained substantial wear throughout the two rounds of testing (.8mm of material lost). It is suggested that if modifications to this design are performed, reversing the material of the bearing and follower sleeve may be more advantageous to reducing the amount of wear to the components.	60
Figure 25: As the trigger is contracted towards the handle, the plunger is advanced up the saddle ramp. This causes the reamer shaft to be translated in one direction instead of deflecting the reamer head at an angle as in previous designs.....	30
Figure 27: The distal end of the plunger contains a 30° incline to mate with the plug at the distal end of the device. The cylindrical feature on the proximal end rests within the trigger flange slots and allows the plunger to be translated forward as the trigger is contracted towards the grip. The rectangular region near the horizontal driving pin is the hard stop feature containing the cavity for the locking ratchet tooth.	31
Figure 28: Shown above is the stainless steel plug and follower sleeve assembly.	32
Figure 26: The proximal components of the directional reamer assembly are shown above. The mating shroud, trigger spring, and ratchet spring, and ball bearings have been omitted for visual clarity.	34
Figure 30: The conical insert was used in the first round of testing at Devicix. Both stainless steel and peek conical inserts were tested.	69
Figure 31: Dimensions for the first follower sleeve prototype are shown above.	69
Figure 32: The 13.25mm conical bearing will be used in conjunction with a 14mm reamer head. This design allows for 3.25mm of lateral cutting.....	70
Figure 33: The flexible follower sleeve for the 14mm head displacement assembly is shown above. The length of the tongue has been increased to allow for greater flexibility along the reamer shaft.....	70
Figure 34: REAMER TORQUE VALUES. Trials 1,2, and 3 were conducted using 10lbs. Trials 4,5, and 6 were conducted using 15lbs. The maximum torque values for each trial did not exceed	

reamer torsional limits (4.63Nm). Data taken during the trials occurs ten seconds into the trial. This delay is due to the time taken to insert the drill into the intramedullary canal. 79

Figure 35: Shown above is the experimental setup for generating a four point bending load on the Stryker flexible reaming shaft. This method of loading allowed the team to isolate the bending stiffness of the flexible shaft (Eqn. 6-8). In order to develop the flexible follower sleeve, this experiment was replicated in SolidWorks 2015 Academic Edition. 80

Figure 36: One of two fixture cuts is shown as the highlighted cylindrical region in the close-up of the follower sleeve in SolidWorks. 82

Figure 37: Lateral view of the deflected cut is located just above the wire ring used to mark the directionally reamed location. 96

Figure 38: (Left) An anterior-posterior view of the femur is shown with the 50% length cut circled in black and the 40% length cut circled in red. (Right) A lateral shot of the deflected cut is shown above. The directionally reamed location is circled in red. 96

Figure 39: (Left) The anterior-posterior view of the directionally reamed location can be seen circled in red just above the wire marker. (Right) The lateral view of the same cut is shown just above the wire marker. 97

Figure 40:(Left) In the anterior-posterior view the reaming assembly was returned to the 50% location to attempt a circumferential cut. (Right) The same cut is shown in the lateral view. Note the reamed material still inside the canal. 97

Figure 41: (Left) Anterior-Posterior image shows the same 50% location of the attempted circumferential cut after the 14mm reamer head had been passed through without deflection in order to clear the reamed debris. (Right) The same location is shown in a lateral view 97

References

1. Trlica, J., et al., *Reamed versus unreamed nail in the treatment of tibia shaft fractures*. European Journal of Trauma and Emergency Surgery, 2013. **40**(4): p. 489-493.
2. Cox, G., et al., *Reamer-irrigator-aspirator indications and clinical results: a systematic review*. Int Orthop, 2011. **35**(7): p. 951-6.
3. Westhauser, F., et al., *Reaming in treatment of non-unions in long bones: cytokine expression course as a tool for evaluation of non-union therapy*. Archives of Orthopaedic and Trauma Surgery, 2015. **135**(8): p. 1107-1116.
4. Takeda, A., et al., *Osteogenic Potential of Human Bone Marrow-Derived Mesenchymal Stromal Cells Cultured in Autologous Serum: A Preliminary Study*. Journal of Oral and Maxillofacial Surgery, 2012. **70**(8): p. e469-e476.
5. Lovisetti, G., et al., *Osteocutaneous thermal necrosis of the leg salvaged by TSF/Ilizarov reconstruction. Report of 7 patients*. International Orthopaedics, 2011. **35**(1): p. 121-126.
6. Hofmann, A., et al., *The role of intramedullary nailing in treatment of open fractures*. European Journal of Trauma and Emergency Surgery, 2015. **41**(1): p. 39-47.
7. Bose, D., et al., *Management of infected nonunion of the long bones by a multidisciplinary team*. Bone & Joint Journal, 2015. **97-B**(6): p. 814.
8. Ehmke, *Femoral Nailing Through the Trochanter: The Reamer Pathway Indicates a Helical Nail Shape*. Journal of Orthopaedic Trauma, 2006. **20**(10): p. 668-674.
9. Egol, K.A., et al., *Mismatch of current intramedullary nails with the anterior bow of the femur*. Journal of Orthopaedic Trauma, 2004. **18**(7): p. 410-5.
10. Wu, C.C., *Treatment of long-bone fractures, malunions, and nonunions: experience at Chang Gung Memorial Hospital, Taoyuan, Taiwan*. Chang Gung Med J, 2006. **29**(4): p. 347-57.
11. Wukich, D.K., et al., *Surgical management of Charcot neuroarthropathy of the ankle and hindfoot in patients with diabetes*. Diabetes/Metabolism Research and Reviews, 2016. **32**: p. 292-296.
12. Lowe, J.A., et al., *Effect of Retrograde Reaming for Tibiotalocalcaneal Arthrodesis on Subtalar Joint Destruction: A Cadaveric Study*. J Foot Ankle Surg, 2016. **55**(1): p. 72-5.
13. Hyer, C.F. and N. Cheney, *Anatomic Aspects of Tibiotalocalcaneal Nail Arthrodesis*. The Journal of Foot and Ankle Surgery, 2013. **52**(6): p. 724-727.
14. Budnar, V.M., et al., *Tibiotalocalcaneal arthrodesis with a curved, interlocking, intramedullary nail*. Foot Ankle Int, 2010. **31**(12): p. 1085-92.
15. Fantry, A.J., et al., *Distal Femoral Complications Following Antegrade Intramedullary Nail Placement*. Orthopedic Reviews, 2015. **7**(1): p. 5820.
16. Carek, P.J., L.M. Dickerson, and J.L. Sack, *Diagnosis and management of osteomyelitis*. Am Fam Physician, 2001. **63**(12): p. 2413-20.
17. Calhoun, J.H., M.M. Manring, and M. Shirtliff, *Osteomyelitis of the Long Bones*. Seminars in Plastic Surgery, 2009. **23**(2): p. 59-72.
18. Gaujoux-Viala, C., et al., *Osteomyelitis in adults: An underrecognized clinical entity in immunocompetent hosts. A report of six cases*. Joint Bone Spine, 2011. **78**(1): p. 75-79.
19. Giannoudis, P., et al., *The effect of IM reaming on the release of growth factors*. Injury Extra, 2007. **38**(4): p. 163.
20. Metsemakers, W.J., et al., *Risk factors for nonunion after intramedullary nailing of femoral shaft fractures: Remaining controversies*. Injury, 2015. **46**(8): p. 1601-1607.

21. Pape, H.-C. and P. Giannoudis, *The biological and physiological effects of intramedullary reaming*. Journal of Bone & Joint Surgery, British Volume, 2007. **89-B**(11): p. 1421-1426.
22. Frölke, J.P.M. and G.C. Reeling Brouwer, *The assessment of cortical heat during intramedullary reaming of long bones*. Injury, 2003. **34**(10): p. 806-807.
23. Hinsenkamp, M. and J.-F. Collard, *Growth factors in orthopaedic surgery: demineralized bone matrix versus recombinant bone morphogenetic proteins*. International Orthopaedics, 2014. **39**(1): p. 137-147.
24. Tang, Y., et al., *TGF- β 1-induced migration of bone mesenchymal stem cells couples bone resorption with formation*. Nat Med, 2009. **15**(7): p. 757-765.
25. Frolke, *Reaming Debris in Osteotomized Sheep Tibiae*. Journal of Trauma-Injury Infection and Critical Care, 2001. **50**(1): p. 65-70.
26. Furlong, A.J., P.V. Giannoudis, and R.M. Smith, *Heterotopic ossification: a comparison between reamed and unreamed femoral nailing*. Injury, 1997. **28**(1): p. 9-14.
27. Kropfl, A., et al., *Intramedullary pressure and bone marrow fat intravasation in unreamed femoral nailing*. J Trauma, 1997. **42**(5): p. 946-54.
28. Ostrum, R.F., et al., *Retrograde intramedullary nailing of femoral diaphyseal fractures*. J Orthop Trauma, 1998. **12**.
29. Canale, S.T., J.H. Beaty, and F.M. Azar, *Campbell's core orthopaedic procedures* 2016, Philadelphia, PA: Elsevier. xvii, 455 pages.